Widespread societal and ecological impacts from projected Tibetan Plateau lake expansion

Xu, Fenglin; Zhang, Guoqing; Woolway, R. Iestyn; Yang, Kun; Wada, Yoshihide; Wang, Jida; Crétaux, Jean-François

Nature Geoscience

DOI:
10.1038/s41561-024-01446-w

Published: 27/05/2024

Peer reviewed version

Widespread societal and ecological impacts from projected Tibetan Plateau lake expansion

Fenglin Xu[1,2], Guoqing Zhang[1✉], R. Iestyn Woolway[3], Kun Yang[4], Yoshihide Wada[5], Jida Wang[6,7], Jean-François Crétaux[8]

[1]State Key Laboratory of Tibetan Plateau Earth System Science, Environment and Resources (TPESER), Institute of Tibetan Plateau Research, Chinese Academy of Sciences, Beijing, China

[2]University of Chinese Academy of Sciences, Beijing, China

[3]School of Ocean Sciences, Bangor University, Menai Bridge, Anglesey, UK

[4]Ministry of Education Key Laboratory for Earth System Modelling, Department of Earth System Science, Tsinghua University, Beijing, China

[5]Biological and Environmental Science and Engineering Division, King Abdullah University of Science and Technology, Thuwal, Saudi Arabia

[6]Department of Geography and Geographic Information Science, University of Illinois Urbana-Champaign, Urbana, Illinois, USA

[7]Department of Geography and Geospatial Sciences, Kansas State University, Manhattan, Kansas, USA

[8]Laboratoire d'Études en Géophysique et Océanographie Spatiales (LEGOS), Université de Toulouse, CNES-IRD-CNRS-UT3, Centre National d'Études Spatiales (CNES), Toulouse, France

✉e-mail: guoqing.zhang@itpcas.ac.cn

Lakes on the Tibetan Plateau are expanding rapidly in response to climate change. The potential impact on the local environment if lake expansion continues remains uncertain. In this study, we integrate field surveys, remote sensing observations, and numerical modelling to assess future changes in lake surface area, water level, and water volume. In addition, we assess the ensuing risks to critical infrastructure, human settlements, and key ecosystem components. Our results suggest that by 2100 even under a low emissions scenario the surface area of endorheic lakes on the Tibetan Plateau will increase by over 50% (~20,000 km^2) and water levels will rise by around 10 m, relative to 2020. This expansion represents approximately a 4-fold increase in water storage compared to 1970s–2020. A shift from lake shrinkage to expansion was projected in the southern plateau around 2021. The expansion is primarily fueled by amplified lake water inputs from increased precipitation and glacier meltwater, profoundly reshaping the hydrological connectivity of the lake basins. In the absence of hazard mitigation measures, lake expansion is projected to submerge critical human infrastructure, including more than 1000 km of roads, approximately 500 settlements, and around 10,000 km^2 of ecological components such as grasslands, wetlands, and croplands. Our study highlights the urgent need for water hazard mitigation and management across the Tibetan Plateau.

Lakes store approximately 87% of the Earth's accessible surface freshwater and play a critical role in global hydrological and biogeochemical cycles[1,2] that are important for ecosystem balance and socio-economic development[3,4]. In recent decades, large lakes around the world have experienced widespread declines in total water storage due to a combination of climate warming and anthropogenic disturbance[5]. In contrast, lakes residing on the Tibetan Plateau (TP) have exhibited an exceptionally dramatic expansion in response to the effects of a warmer and wetter climate[6-8]. As such, lake changes within the TP have received considerable attention in studies of global climate change[9,10].

The TP, often referred to as the "Earth's Third Pole", contains vast stores of both solid (glaciers and permafrost) and liquid (lakes) water[11]. It is also one of the most vulnerable regions to climate change, acting as an early warning signal for the wider effects of global warming[12,13]. The TP has experienced a remarkable expansion of lakes, and the spatial difference is evident[10,14]. The TP is also witnessing a greener and more habitable environment, with a growing population seeking refuge at higher altitudes due to the benefits of warming-induced accessibility to water resources[15,16]. However, the continued expansion of lakes is leading to potential basin mergers or reorganizations, threatening the region's infrastructure and ecological security (Fig. 1, Extended Data Fig. 1). Despite the existence of some models to study future changes in the surface area and water storage of the TP's endorheic lakes, their applicability to specific lakes remains uncertain due to the spatio-temporal heterogeneity. Some models have focused on specific large lakes or single case studies but fail to encompass comprehensive future lake changes and their broader impacts on the TP[17-20].

In this study, we address these knowledge gaps by developing a generalized data-driven modelling framework that integrates the key drivers (precipitation, glacier meltwater, land surface evapotranspiration, and lake evaporation) (Extended Data Fig. 2) and incorporates field surveys and remote sensing observations. We quantify the annual changes in area, water level, and storage of individual endorheic lakes from 2021 to 2100 under Shared Socioeconomic Pathways (SSPs) scenarios. We then assess the magnitude of the impacts on lake basin reorganization, infrastructure, and the ecological environment. We highlight the need to develop effective strategies to mitigate water hazards, while protecting biodiversity and safeguarding the well-being of people living in this ecologically sensitive region.

Future changes in lake area and water storage

The future surface area of endorheic lakes on the TP are projected to increase to 53,657±5,068 (+52% compared to the area in 2020, ~2303 km^2/dec), 54,311±5,308 (+54%, ~2385 km^2/dec), and 58,716±6,681

(+67%, ~2936 km^2/dec) km^2 by 2100 under the SSP1-2.6, SSP2-4.5, and SSP5-8.5 scenarios, respectively (Fig. 2a). Accompanying the expansion of lake surface area, water levels are projected to rise by 10.21±4.14 m (~1.28 m/dec) under SSP1-2.6, 10.64±4.33 m (~1.33 m/dec) under SSP2-4.5, and 13.29±5.18 m (~1.66 m/dec) under SSP5-8.5 scenarios by 2100 (Fig. 2b). The future rates of lake surface area expansion and water level rise are expected to slow down substantially, compared to an increase in lake area of ~11,400 km^2 and a rise in water level of ~5.25 m between 2000 and 2020, respectively[21]. Over the next 80 years, lake water storage is estimated to increase by 652.97±211 (~81.50 Gt/dec), 665.32±220 (~83.13 Gt/dec), and 908.44±282 (~113.50 Gt/dec) Gt, under the SSP1-2.6, SSP2-4.5, and SSP5-8.5 scenarios, respectively, which are ~3.9, ~3.9 and ~5.4 times the increase in water storage between 2000 and 2020, respectively (Fig. 2c). However, this change in water storage by 2100 is a staggering ~4-fold increase compared to the 1970s–2020 period.

Our analysis shows a pronounced heterogeneity in the spatial distribution of future lake changes (Fig. 2, Extended Data Figs. 3–4, Supplementary Figs. S1–S2). The most significant change is observed in the northern TP, where the total lake area is projected to increase two-fold by 2100 under the SSP5-8.5 scenario. Albeit to a lesser extent, lakes in the southeastern, central, and northwestern endorheic TP are expected to expand significantly (51–71%). Historically, lake changes in the southern TP have followed a shrinking trend[10,22]. However, our projections indicate a remarkable transition from shrinkage to expansion in ~2021 (Extended Data Fig. 4, Supplementary Figs. S1–S3).

There are notable differences in the evolution of lake surface area, water level, and water storage. During the period 2021–2100, changes in lake storage (level and area) range from about -0.61 Gt (corresponding to -11.89 m and -8 km^2) to 66 Gt (59 m and 903 km^2). Most of the increases are between ~0.86 Gt (3.96 m and 7.83 km^2, 25th percentile) and ~1.29 Gt (14.21 m and 47.14 km^2, 75th percentile). Notably, Selin Co, the largest lake in Tibet and the second largest lake in the TP, exhibits the largest substantial water gain of ~66 Gt along with corresponding increases in area of ~800 km^2 and level of ~21 m under the SSP2-4.5 scenario.

Changes in the hydrological connectivity of lake basins

Under the SSP1-2.6, SSP2-4.5, and SSP5-8.5 scenarios, 70 (23%), 70 (23%), and 79 (26%) lake basins will be reorganized into 28, 28, and 31 basins respectively by 2100 (Fig. 3a). New reorganizations will occur mainly in the northern, eastern, and southern endorheic TP (Fig. 3c). In addition, 21, 19, and 23 lakes will merge (i.e., two or more lakes merging into one) under these scenarios, forming 10, 9, and 11 lakes, respectively (Fig. 3b). Lake mergers are predicted to occur mainly in the northeastern and southeastern TP (Fig. 3d). With the anticipated growth of lakes in the future, the reconfiguration of the drainage system, spurred by the interconnected nature of these lakes, is expected to become even more extensive.

Seven different types of basin reorganizations are identified, each characterized by distinct processes, quantities, and types of lakes (endorheic and exorheic) (Extended Data Fig. 5). In the future, most basin reorganizations are projected to follow cascading overflow (Type I), and the progression from the amalgamation of endorheic lakes (Type II) to the inflow of lakes into a merged basin (Type III) will occur when merged lakes experience overflow. The outflow of a merged basin into a lake (Type IV) and the convergence of several lakes into a single basin (Type V) are less common, with only one reorganized basin in each case. In addition, future lake expansion can lead to shifts in lake type, such as an endorheic lake becoming exorheic (Type VI). The confluence of endorheic and exorheic lakes (Type VII) shows a particular type of merging, where three endorheic and two exorheic lakes merge into one endorheic lake. Different reorganization types could occur for the same lake over different time periods, given the intricate dynamics of continuous expansion. The future evolution of lakes is thus poised to be very complex.

Impact of future lake expansion

By the end of this century, 1023±281, 959±274 and 1481±421 km of roads will be inundated under the SSP1-2.6, SSP2-4.5, and SSP5-8.5 scenarios, respectively, (Fig. 4a). Under the SSP2-4.5 (SSP1-2.6 and SSP5-8.5) scenarios, ~118 (149 and 136), 215 (264 and 258), and 331 (382 and 390) km of roads are still at risk of flooding in 2030, 2040, and 2050, respectively. The inundated roads are mainly concentrated in the southern endorheic TP. Despite the most significant lake expansion in the northern endorheic TP, the presence of seasonal permafrost limits road construction and human access, resulting in fewer flooded roads. Conversely, although lake expansion is less in the northeastern TP (Fig. 2, Extended Data Fig. 4), a significant number of road segments are expected to be inundated due to increased human activity and the prevalence of roads adjacent to lakes (Extended Data Fig. 6). At the lake scale, 12 lakes including the three largest lakes (Selin Co, Nam Co, and Qinghai Lake) are identified as potentially more vulnerable (Extended Data Fig. 7). Selin Co has the most submerged roads, with the projected length of submerged roadways expected to reach about 84.13–119.08 km by 2100. Due to the rapid expansion of Selin Co, the S208 highway was broken by the outflow flood at the end of September 2023 (Fig. 5). Nam Co, which is almost surrounded by roads, is expected to have ~73.27, ~34.02, and ~118.91 km of roads submerged under the three scenarios, respectively. Due to the significant expansion of Qinghai Lake, some roads in the northwest have been inundated (Fig. 5). Approximately 46.9 km of road is expected to be inundated under the SSP5-8.5 scenario. In summary, a significant number of roads are potentially at risk of being submerged by future lake expansion, which is a serious threat that should be considered in future rail and road planning.

Given the importance of water resources and religious culture in the TP, many settlements such as villages, herders' houses, and livestock pens are located around lakes (Fig. 1, Extended Data Fig. 1a). Projections indicate that by the year 2100, an estimated 5.66, 7.40 and 5.78 million people will inhabit in the TP under the SSP1-2.6, SSP2-4.5, and SSP5-8.5 scenarios, respectively[23]. Approximately 462, 458, and 615 settlements will be inundated, respectively, and most of them are in the southern endorheic TP (Fig. 4b, Extended Data Fig. 6). Moreover, between 83 and 93 lakes are anticipated to inundate settlements, with Selin Co posing the greatest risk, inundating 64 to 81 settlements across various SSP scenarios. Notably, certain settlements already face inundation or are at heightened risk, such as the village and building near Zhari Namco and Padu Co (Fig. 5), and this impending threat is expected to increase in the future.

The future expansion of TP lakes will also inundate many ecological components, including grasslands, wetlands, croplands, forests, and sparse vegetation (Figs. 4–5, Supplementary Fig. S4). By the year 2100, the anticipated inundation areas are projected to reach 8,533, 9,132, and 11,576 km^2 by 2100 under the SSP1-2.6, SSP2-4.5, and SSP5-8.5 scenarios, respectively. More than ~500,000 head of livestock could be disturbed, assuming even distribution of livestock (Supplementary Fig. S5). 4,241±1168, 4,459±1241, and 5,968±1823 km^2 of grassland will be inundated by 2100 in the SSP scenarios, respectively (Fig. 4c). This will directly lead to a decline in livestock production, severely affecting the livelihoods of local pastoralists and further exacerbating poverty levels. We also identified 291 lakes widely distributed across the plateau, which pose a threat to the security of the grasslands (Fig. 4c), such as the large grasslands near Peng Co (Fig. 5). Loss of cropland could disrupt food production, affecting both local food security and the regional agricultural economy.

Implications and mechanisms of future lake expansion

As lakes on the TP continue to expand, there is growing concern about increased emissions of greenhouse gases, including carbon dioxide and methane, into the atmosphere[24]. These emissions can further exacerbate global warming, creating a positive feedback loop that amplifies the effects of climate change. In addition, the submergence of grasslands due to flooding can lead to the decomposition of organic matter, releasing additional carbon dioxide into the atmosphere[25]. Furthermore, the interaction between these lakes and the atmosphere, as well as their role in regional hydrological cycles such as extreme rainfall or snowfall events[26,27], is expected to intensify as lakes expand in size in the future.

Future increases in lake water volume, with an increase influx of freshwater, can lead to decreases in salinity[28,29], which could substantially impact the physical environment of lakes[30,31], alter species richness, composition, and the trophic structure of lake ecosystems[32]. Rising lake surface water temperatures and increasing heatwaves have cascading effects on the physical structure and chemical properties of aquatic systems, threatening lake biodiversity[33,34]. In addition, the overflow water carrying eroded sediments will increase the turbidity and sedimentation in the receiving lakes[35], which could disrupt the ecological balance of the lakes and lead to species loss. The newly formed channels resulting from lake basin reorganization and lake merging can lead to a cascade of hydrogeomorphic processes along their paths, such as incision, lateral erosion or aggradation, thermal erosion, and increased infiltration, which affect the regional ecological environment and disrupt ecological migration. For example, Zonag Lake in Hoh Xil Nature Reserve burst in September 2011, blocking the Tibetan antelope migration route and affecting their survival and reproduction[36]. The effects of this drainage reorganization can spill over into larger downstream basins.

From a socio-economic perspective, the direct economic loss due to inundated roads by 2100 under the SSP2-4.5 scenario, is estimated at RMB 20 to 50 billion based on investment costs in 2022[37]. The future expansion of lakes can enhance the natural landscapes and increase sustainable tourism development and local income. The Tibet Autonomous Region plans to build ~5,600 km of new highways and three railways[37] (Supplementary Fig. S6). The expanding lakes pose challenges to existing and planned infrastructure and communities and require urgent implementation of effective adaptation and sustainable management strategies to mitigate socio-economic repercussions.

Glacier meltwater contributes ~9% to the increase in lake storage from 1995 to 2020[38], and although the temperature of the TP will continue to rise, the contribution of glacier meltwater is estimated to be only 7–15% by 2100 (Extended Data Fig. 8), due to the limited storage of the remaining glaciers[39,40-42]. Lake evaporation is also an important driver of water loss, and the reduction in lake ice this century is likely to lead to an increase in lake evaporation[43,44], but the relative contribution is small[19], with an estimated loss contribution of about -34% under SSP2-4.5 and SSP5-8.5 scenarios. Due to future increases in temperature and radiation, precipitation is likely to remain the main controlling factor for evapotranspiration on the TP[45]. Lake expansion on the TP is primarily influenced by net precipitation[7,22,46], and the significant increase in future net precipitation will act as a greater water gain leading to further lake expansion, with an estimated relative contribution of 109 – 116%.

Given the current context of global warming and climate change, it is crucial to comprehensively understand the future changes of the lakes to effectively manage water resources, mitigate hazards, and preserve the ecology of this crucial region. Our study serves as a scientific guide for future planning and provides valuable insights to avoid the devastating consequences of the impending lake expansion.

Acknowledgements

This study was supported by grants from the Second Tibetan Plateau Scientific Expedition and Research Program (2019QZKK0201), and Basic Science Center for Tibetan Plateau Earth System (BSCTPES, NSFC project no. 41988101-03). RIW was supported by a UKRI Natural Environment Research Council (NERC) Independent Research Fellowship [grant number NE/T011246/1] and a NERC grant reference number NE/X019071/1, "UK EO Climate Information Service". Contribution of JFC was funded by the ESA Climate Change Initiative project on the Lake Essential Variables (Contract No 4000125030/18/I-NB).

Author contributions

G.Z. designed the study. F.X. and G.Z. drafted the manuscript. R.I.W., K.Y., Y.W., J.W. and J.F.C. edited the manuscript. All authors contributed to the final form of the study.

Competing interests

The authors declare no competing interests.

Figure Legends/Captions:

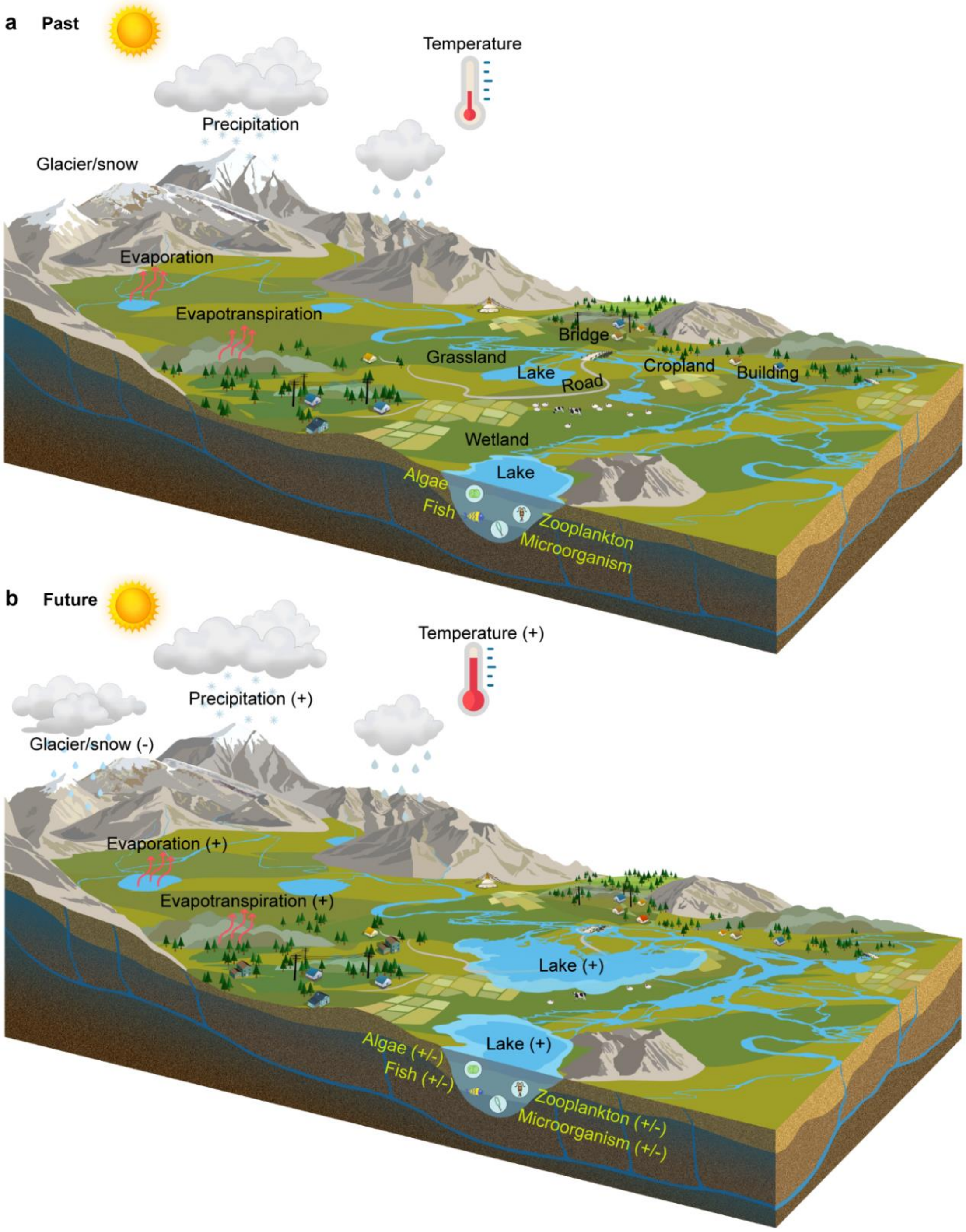

Fig. 1|Schematic diagram illustrating future lake development and impacts over the TP. a, Past lake status. **b**, Future lake development and impacts. Expansion of lake boundaries and changes in the hydrological connectivity of lake basins are the result of increased net precipitation and glacier/snow melt. Future lake expansion will result in threats to human infrastructure such as roads and settlements, and ecological components such as grasslands, wetlands, and croplands, as well as changes to the lake ecosystem such as algae, fish, zooplankton, microorganism. Credit: Temperature and evaporation icons in **a** and **b**, Flaticon.com.

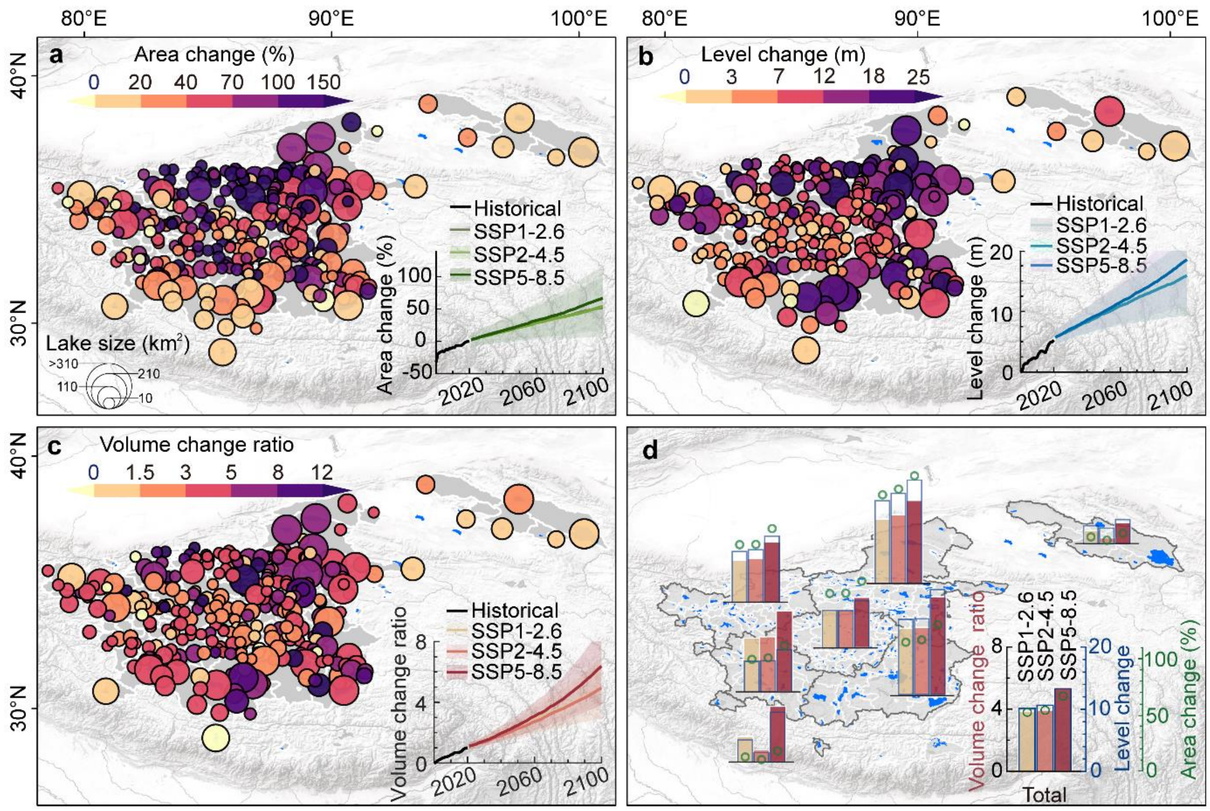

Fig. 2|The spatial patterns of lake surface area, water level, and storage changes between 2020 and 2100 under the SSP2-4.5 scenario. a, The percentage of lake area change in 2100 relative to 2020. **b**, The lake level change in 2100 relative to 2020. **c**, The ratio of lake storage change between 2020 and 2100 relative to the change between 2000 and 2020. The insets in **a**, **b** and **c** show the evolution trends of all lakes under the SSP1-2.6 to SSP5-8.5 scenarios, and the range of the error bands shows the 95% confidence intervals of the estimations of the bootstrap method. **d**, The changes in lake area, water level, and storage in each subregions. Additional SSP1-2.6 and SSP25-8.5 scenarios are shown in Extended Data Fig. 3.

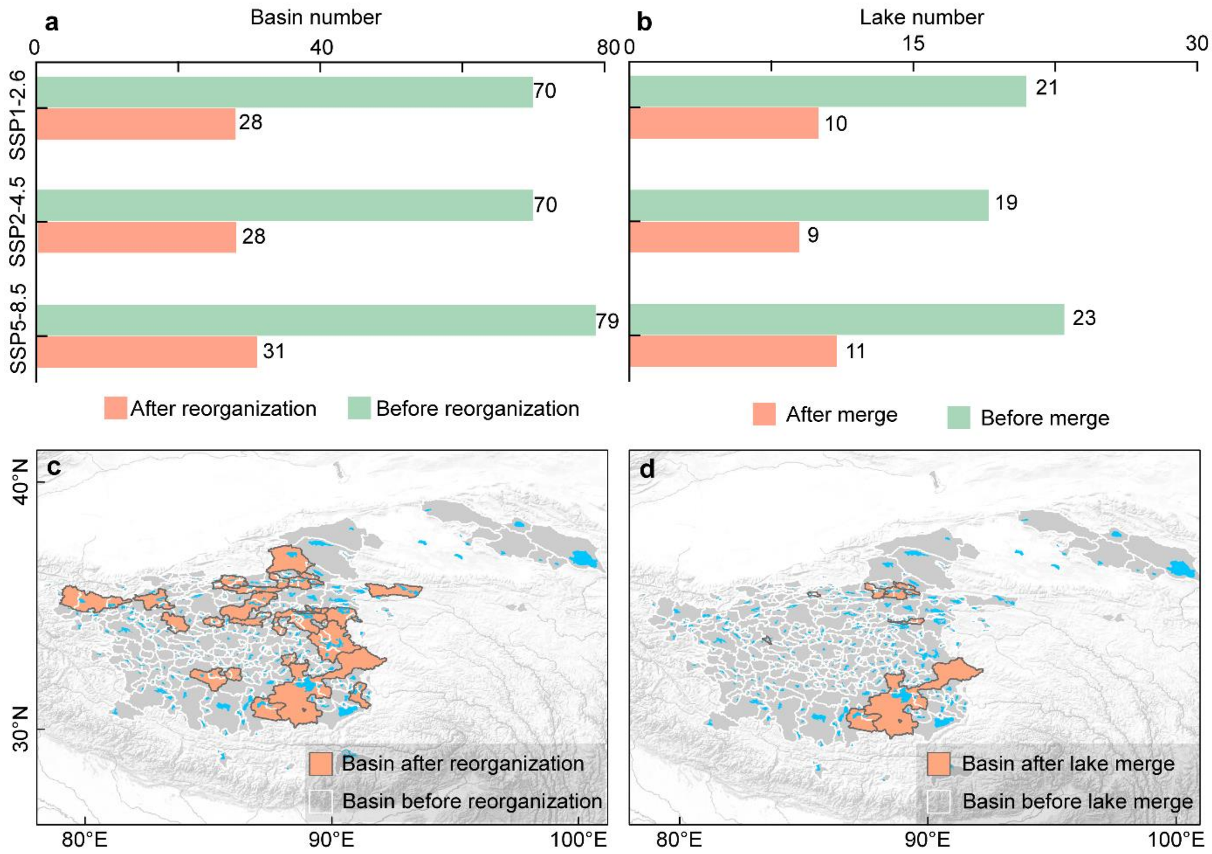

Fig. 3|Future reorganization of lake basins and lake mergers. **a,** Number of basins before and after reorganization under different scenarios. **b,** Number of lakes before and after mergers under different scenarios. **c,** Spatial distribution of basin reorganization under the SSP2-4.5 scenario. **d,** Spatial distribution of lake mergers under the SSP2-4.5 scenario. The merged lakes are shown as merged basins because each lake basin has only one endorheic lake.

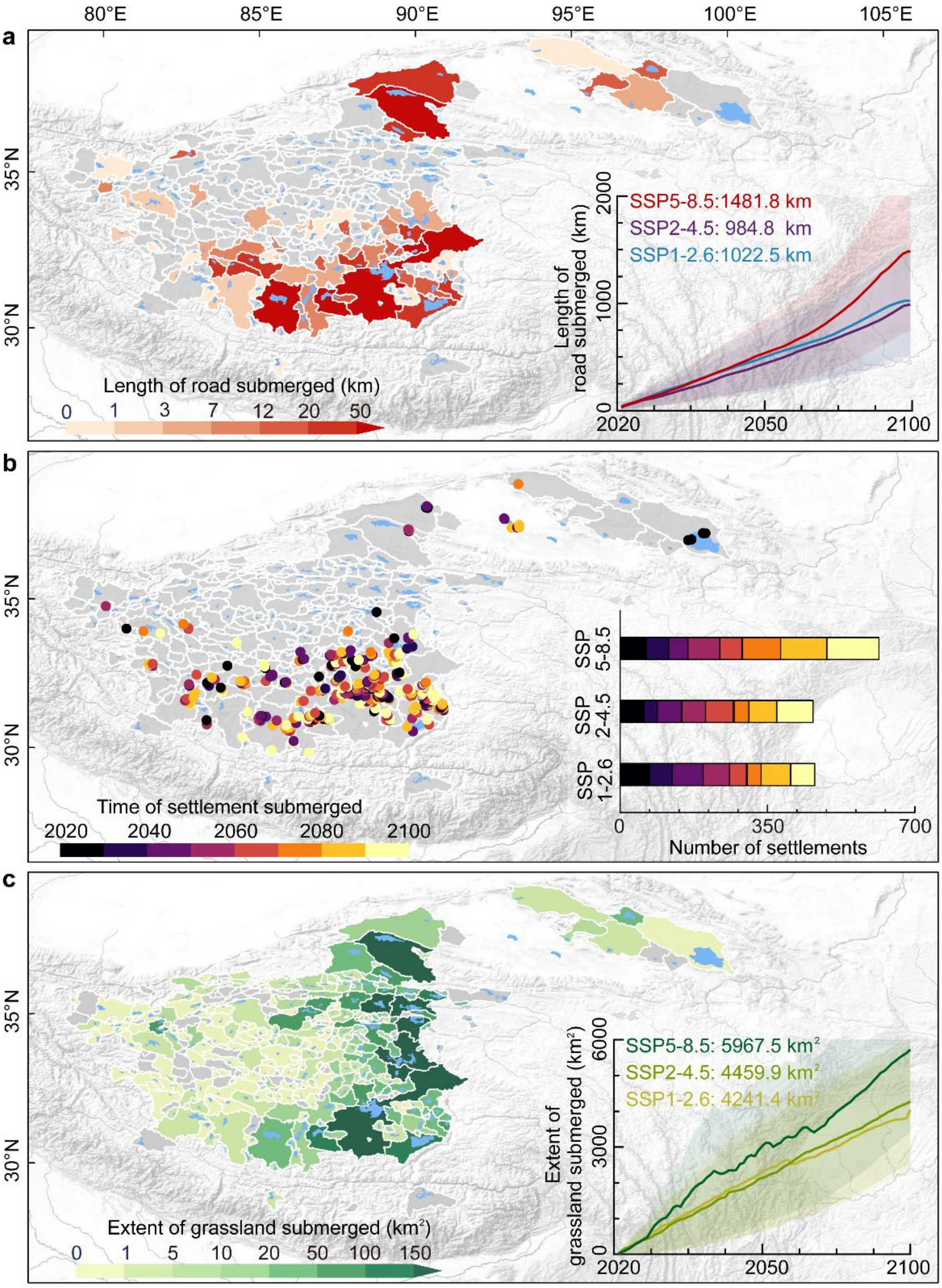

Fig. 4|The roads, settlements, and grasslands submerged by expanding lakes by 2100 under the SSP2-4.5 scenario. **a**, Spatial distribution of the length of submerged roads across the lake basin. **b**, Spatial distribution and time of submerged settlements. **c**, Spatial distribution of the extent of submerged grasslands. Insets show annual variations in the length of submerged roads (**a**), the number of submerged settlements (**b**), and annual variations in the extent of submerged grasslands (**c**) under different climate scenarios, with the range of the error bands estimated based on 95% confidence intervals for the lake area. Additional SSP1-2.6 to SSP5-8.5 scenarios are shown in Extended Data Fig. 6.

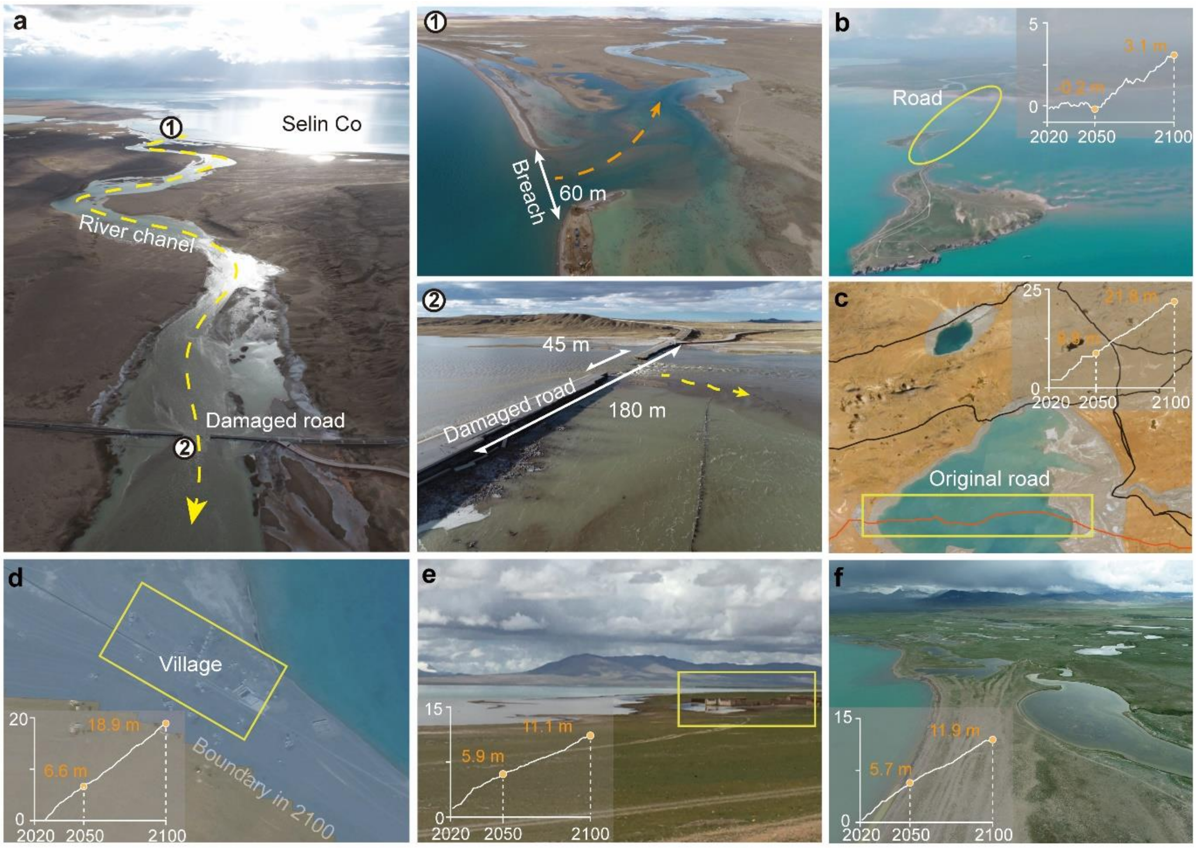

Fig. 5|Cases of roads, bridges, settlements, and grasslands threatened by expanded lakes. a, The S208 road was damaged by flooding due to Selin Co expansion on around 25 September 2023. Field photos taken by F. Xu on 2 October, 2023. **b**, Roads indundated by Qinghai Lake expansion. **c**, Original S301 road (red) indundated and roads potentially indundated. **d**, Village at high risk near Zhari Namco. **e**, Settlement indundated near Padu Co. Photos were taken by R. Zhang. **f**, High-risk grasslands near Peng Co. The insets show the evolution of lake levels under the SSP1-2.6 scenario. The location of these lakes is indicated in Extended Data Fig. 1.

References

1 Williamson, C. E., Saros, J. E., Vincent, W. F. & Smol, J. P. J. L. Lakes and reservoirs as sentinels, integrators, and regulators of climate change. *Limnology and Oceanography* **54**, 2273-2282, doi:10.4319/lo.2009.54.6_part_2.2273 (2009).

2 Raymond, P. A. *et al.* Global carbon dioxide emissions from inland waters. *Nature* **503**, 355-359, doi:10.1038/nature12760 (2013).

3 Reynaud, A. & Lanzanova, D. A Global Meta-Analysis of the Value of Ecosystem Services Provided by Lakes. *Ecol Econ* **137**, 184-194, doi:10.1016/j.ecolecon.2017.03.001 (2017).

4 Loewen, C. J. G. Lakes as model systems for understanding global change. *Nature Climate Change* **13**, 304-306, doi:10.1038/s41558-023-01624-5 (2023).

5 Yao, F. *et al.* Satellites reveal widespread decline in global lake water storage. *Science* **380**, 743-749,

doi:10.1126/science.abo2812 (2023).

6 Pekel, J. F., Cottam, A., Gorelick, N. & Belward, A. S. High-resolution mapping of global surface water and its long-term changes. *Nature* **540**, 418-422, doi:10.1038/nature20584 (2016).

7 Zhang, G. Q. *et al.* Lake volume and groundwater storage variations in Tibetan Plateau's endorheic basin. *Geophysical Research Letters* **44**, 5550-5560, doi:10.1002/2017gl073773 (2017).

8 Yao, F. *et al.* Lake storage variation on the endorheic Tibetan Plateau and its attribution to climate change since the new millennium. *Environmental Research Letters* **13**, doi:10.1088/1748-9326/aab5d3 (2018).

9 Woolway, R. I. *et al.* Global lake responses to climate change. *Nature Reviews Earth & Environment* **1**, 388-403, doi:10.1038/s43017-020-0067-5 (2020).

10 Zhang, G. *et al.* Response of Tibetan Plateau lakes to climate change: Trends, patterns, and mechanisms. *Earth-Science Reviews* **208**, doi:10.1016/j.earscirev.2020.103269 (2020).

11 Yao, T. *et al.* The imbalance of the Asian water tower. *Nature Reviews Earth & Environment* **3**, 618-632, doi:10.1038/s43017-022-00299-4 (2022).

12 Chen, D. *et al.* Assessment of past, present and future environmental changes on the Tibetan Plateau. *Chinese Science Bulletin* **60**, 3025-3035, doi:10.1360/n972014-01370 (2015).

13 Immerzeel, W. W. *et al.* Importance and vulnerability of the world's water towers. *Nature* **577**, 364-369, doi:10.1038/s41586-019-1822-y (2019).

14 Ma, R. *et al.* A half-century of changes in China's lakes: Global warming or human influence? *Geophysical Research Letters* **37**, L24106, doi:10.1029/2010gl045514 (2010).

15 Zhang, W., Zhou, T. & Zhang, L. Wetting and greening Tibetan Plateau in early summer in recent decades. *Journal of Geophysical Research: Atmospheres* **122**, 5808-5822, doi:10.1002/2017jd026468 (2017).

16 Zhong, L., Ma, Y., Xue, Y. & Piao, S. Climate Change Trends and Impacts on Vegetation Greening Over the Tibetan Plateau. *Journal of Geophysical Research: Atmospheres* **124**, 7540-7552, doi:10.1029/2019jd030481 (2019).

17 Jia, B., Wang, L. & Xie, Z. Increasing lake water storage on the Inner Tibetan Plateau under climate change. *Science Bulletin* **68**, 489-493, doi:10.1016/j.scib.2023.02.018 (2023).

18 Adnan, M. *et al.* Prediction of changes in water balance of Nam Co Lake under projected climate change scenarios. *Hydrological Sciences Journal* **66**, 1712-1727, doi:10.1080/02626667.2021.1957474 (2021).

19 Yang, K. *et al.* Quantifying recent precipitation change and predicting lake expansion in the Inner Tibetan Plateau. *Climatic Change* **147**, 149-163, doi:10.1007/s10584-017-2127-5 (2018).

20 Cheng, J. *et al.* Regional assessment of the potential risks of rapid lake expansion impacting on the Tibetan human living environment. *Environmental Earth Sciences* **80**, doi:10.1007/s12665-021-09470-4 (2021).

21 Zhang, G., Bolch, T., Chen, W. & Cretaux, J. F. Comprehensive estimation of lake volume changes on the Tibetan Plateau during 1976-2019 and basin-wide glacier contribution. *Sci. Total Environ.* **772**, 145463, doi:10.1016/j.scitotenv.2021.145463 (2021).

22 Lei, Y. *et al.* Response of inland lake dynamics over the Tibetan Plateau to climate change. *Climatic Change* **125**, 281-290, doi:10.1007/s10584-014-1175-3 (2014).

23 Chen, Y. *et al.* Provincial and gridded population projection for China under shared socioeconomic pathways from 2010 to 2100. *Sci Data* **7**, 83, doi:10.1038/s41597-020-0421-y (2020).

24 Pi, X. *et al.* Mapping global lake dynamics reveals the emerging roles of small lakes. *Nat Commun* **13**, 5777, doi:10.1038/s41467-022-33239-3 (2022).

25 Marcé, R. *et al.* Emissions from dry inland waters are a blind spot in the global carbon cycle. *Earth-Science Reviews* **188**, 240-248, doi:10.1016/j.earscirev.2018.11.012 (2019).

26 Su, D. *et al.* Simulation of the potential impacts of lakes on glacier behavior over the Tibetan Plateau in

summer. *Climate Dynamics* **60**, 3435-3454, doi:10.1007/s00382-022-06517-5 (2022).
27 Yao, X. *et al.* Surface friction contrast between water body and land enhances precipitation downwind of a large lake in Tibet. *Climate Dynamics* **56**, 2113-2126, doi:10.1007/s00382-020-05575-x (2021).
28 Liu, C. *et al.* In-situ water quality investigation of the lakes on the Tibetan Plateau. *Science bulletin* **66**, 1727-1730, doi:10.1016/j.scib.2021.04.024 (2021).
29 Song, C. *et al.* Widespread declines in water salinity of the endorheic Tibetan Plateau lakes. *Environmental Research Communications* **4**, doi:10.1088/2515-7620/ac9351 (2022).
30 Boehrer, B. & Schultze, M. Stratification of lakes. *Reviews of Geophysics* **46**, doi:10.1029/2006rg000210 (2008).
31 Ladwig, R., Rock, L. A. & Dugan, H. A. Impact of salinization on lake stratification and spring mixing. *Limnology and Oceanography Letters* **8**, 93-102, doi:10.1002/lol2.10215 (2021).
32 Lin, Q. *et al.* Responses of trophic structure and zooplankton community to salinity and temperature in Tibetan lakes: Implication for the effect of climate warming. *Water Res* **124**, 618-629, doi:10.1016/j.watres.2017.07.078 (2017).
33 Woolway, R. I. *et al.* Lake heatwaves under climate change. *Nature* **589**, 402-407, doi:10.1038/s41586-020-03119-1 (2021).
34 Wang, X. *et al.* Climate change drives rapid warming and increasing heatwaves of lakes. *Science Bulletin* **68**, 1574-1584, doi:10.1016/j.scib.2023.06.028 (2023).
35 Lu, S. *et al.* Drainage basin reorganization and endorheic-exorheic transition triggered by climate change and human intervention. *Global and Planetary Change* **201**, doi:10.1016/j.gloplacha.2021.103494 (2021).
36 Pei, J. *et al.* Recovered Tibetan antelope at risk again. *Science* **366**, 194-194, doi:10.1126/science.aaz2900 (2019).
37 *Department of Transport of Tibet Autonomous Region*, <https://jtt.xizang.gov.cn> (2023).
38 Chen, W. *et al.* What Controls Lake Contraction and Then Expansion in Tibetan Plateau's Endorheic Basin Over the Past Half Century? *Geophysical Research Letters* **49**, e2022GL101200, doi:10.1029/2022gl101200 (2022).
39 Huss, M. & Hock, R. J. N. C. C. Global-scale hydrological response to future glacier mass loss. *Nature Climate Change* **8**, 135-140, doi:10.1038/s41558-017-0049-x (2018).
40 Rounce, D. R. *et al.* Global glacier change in the 21st century: Every increase in temperature matters. *Science* **379**, 78-83, doi:10.1126/science.abo1324 (2023).
41 Hugonnet, R. *et al.* Accelerated global glacier mass loss in the early twenty-first century. *Nature* **592**, 726-731, doi:10.1038/s41586-021-03436-z (2021).
42 Rounce, D. R., Hock, R. & Shean, D. E. Glacier Mass Change in High Mountain Asia Through 2100 Using the Open-Source Python Glacier Evolution Model (PyGEM). *Frontiers in Earth Science* **7**, 331, doi:10.3389/feart.2019.00331 (2020).
43 Wang, X. *et al.* Continuous Loss of Global Lake Ice Across Two Centuries Revealed by Satellite Observations and Numerical Modeling. *Geophysical Research Letters* **49**, doi:10.1029/2022gl099022 (2022).
44 Sharma, S. *et al.* Widespread loss of lake ice around the Northern Hemisphere in a warming world. *Nature Climate Change* **9**, 227-231, doi:10.1038/s41558-018-0393-5 (2019).
45 Ma, N. & Zhang, Y. Increasing Tibetan Plateau terrestrial evapotranspiration primarily driven by precipitation. *Agricultural and Forest Meteorology* **317**, doi:10.1016/j.agrformet.2022.108887 (2022).
46 Tong, K., Su, F. & Xu, B. Quantifying the contribution of glacier meltwater in the expansion of the largest lake in Tibet. *Journal of Geophysical Research: Atmospheres* **121**, doi:10.1002/2016jd025424 (2016).

Methods

Historical lake storage changes

Weekly to annual historical changes in lake water storage from five data sources were used to project as many lakes as possible (Supplementary Table S1): (1) Hydroweb (http://hydroweb.theia-land.fr/hydroweb)[47,48], which contains time series of lake water level, surface area and storage changes, and hypsometric curves, covering 42 endorheic lakes in the TP; (2) Annual area and water storage of 976 lakes large than 1 km^2 on the TP for 1991–2018[49]; (3) Annual area of ~300 lakes larger than 10 km^2 in the TP for 1991–2018 and hypsometric curve[7]; (4) Water storage changes for 1132 lakes with ~5 year interval and hypsometric curve[21]; (5) Weekly to monthly water level and storage changes for 52 lakes on the TP during 2000–2017 and hypsometric curve[50]. These different types of datasets, that convert area or water level to water storage change by combining hypsometric curves were integrated. In this study, 307 lakes representing ~97% of the total area of endorheic lakes in the TP were selected based on the availability of historical annual lake volume change.

Precipitation product

The average of two sets of historical precipitation products including ERA5-Land and TPHiPr was used (Supplementary Table S2). ERA5-Land, a state-of-the-art reanalysis precipitation, is an enhanced global dataset for the land component of the fifth generation of European ReAnalysis (ERA5) produced by the European Centre for Medium-Range Weather Forecasts (ECMWF)[51], spanning 1950 to the present, with hourly to monthly resolution. ERA5-Land data with a spatial resolution of ~9 km is interpolated from the ERA5 data with a spatial resolution of ~31 km, using a linear interpolation method based on a triangular mesh. Although ERA5-Land overestimates the amount of precipitation, it provides a good representation of the spatio–temporal variation patterns over the TP[52]. TPHiPr is a high-precision precipitation dataset for the Third Pole region (1/30°, daily), obtained by merging the atmospheric simulation-based ERA5_CNN product with over 9000 rain gauges, using the climatologically aided interpolation and random forest methods[53]. This dataset has better accuracy compared to ERA5-Land, IMAGE, MSWEP v2 and AERA5-Asia data, with a Root Mean Square Error (RMSE) of 5.0 mm d^{-1}. The comparison of precipitation time series between TPHiPr and ERA5-Land (Supplementary Fig. S7), suggested a good agreement. Importantly, the offset between these two datasets did not contribute to uncertainties, as the precipitation anomaly served as the basis for lake modelling. However, we used the average of TPHiPr and ERA5-Land to minimize the uncertainty of the lake projections. For the future precipitation product, the monthly outputs of the 32 CMIP6 ESMs under the SSP1-

2.6, SSP2-4.5 and SSP5-8.5 scenarios were used and calibrated against ERA5-Land and TPHiPr data, respectively, during the overlap period. The top 15 ESMs in each basin were selected using historical references from ERA5-Land and TPHiPr data, respectively, and subsequently the ensemble mean of the 30 ESMs served as future precipitation. Further details on the downscaling and selection for the CMIP6 ESMs method are available in the Supplementary Text1 (Supplementary Figs. S8–9). Detailed information on the evapotranspiration product and glacier mass balance data used in this study can be found in the Supplementary Texts2–3.

Lake evaporation forcing data

The forcing variables were used to calculate evaporation include air temperature, specific humidity, pressure, downward shortwave radiation, downward longwave radiation, and wind speed. These variables were obtained from the China Meteorological Forcing Dataset (CMFD) with a 3-hour time step and grid resolution of 0.1°[54], and bias-corrected CMIP6 ESM. It should be noted that although CMFD is considered to be the most accurate meteorological data for the TP, errors have been identified based on observed data. Therefore, linear corrections were applied to air temperature, specific humidity, air pressure, downward shortwave radiation and wind speed using correction equations from the previous studies[55,56], which could reduce the bias of the CMFD. Details on the corrections equation are available in the Supplementary Text4. The bias-corrected CMFD was then used to correct the CMIP6 15–36 ESMs. For each lake, the area-weighted mean of the forcing data was calculated for the grids intersecting each lake. Further details on the downscaling for CMIP6 ESM method are available in the Supplementary Text1.

Estimate of lake surface evaporation

During the unfrozen period, the monthly lake evaporation rates were calculated using the Penman-Monteith equation (Eq. 1), which is widely used to estimate open water evaporation[57-59].

$$E_w = \frac{\Delta}{\Delta+\gamma}\frac{R_n}{\lambda} + \frac{\gamma}{\Delta+\gamma}E_a \quad (1)$$

where Ew is the daily evaporation rate (mm day^{-1}); Rn represents the net radiation (W/m^2); Δ is the slope of the saturated vapour pressure curve (kPa °C^{-1}); γ is the psychrometric constant (kPa °C^{-1}); λ is the latent heat of vaporization (2.45 MJ kg^{-1}).

Ea (mm day^{-1}) denotes the evaporative component from the turbulent movement of water vapour by eddy diffusion[60] and as follows:

$$E_a = 0.26(1 + 0.54u)(e_s - e_a) \quad (2)$$

where u is the wind speed at 2 m; $es{-}ea$ is the vapour pressure deficit (VPD) (KPa). During the freeze period, lake evaporation is in the form of sublimation and is estimated by the equation (Eq. 2)[61]. Further details on the historical and future lake ice phenology are available in the Supplementary Text5.

Net radiation (Rn) over the lake surface was estimated using (Eq. 3):

$$R_n = (1 - \alpha)K^{\downarrow} + L^{\downarrow} - L^{\uparrow} \quad (3)$$

where α is the lake surface albedo (0.07); $K^{\downarrow}$ is the downward shortwave radiation (W/m^2); $L^{\downarrow}$ is the downward longwave radiation (W/m^2); $L^{\uparrow}$ is the estimated upward longwave radiation (W/m^2) using $L^{\uparrow} = \varepsilon_w \sigma (T_a + 273.15)^4$; Ta denotes air temperature, which ideally should be the lake surface temperature, but due to the unavailability of future data, air temperature is used as a proxy. As we use the relative change in evaporation, the effect of this term on the evaporation is minimal.

Development of future lake modelling framework

Future lake modelling is limited by the following factors: (1) region-specific methods exist, but individual lake-specific modelling methods for large scales are lacking[19]; (2) the limitation of large-scale application of land surface or hydrological models due to the scarcity of runoff inflow observations for lakes (available only for Selin Co and Nam Co)[18]; (3) without considering the topography constraints on future lake changes and hydrological connectivity between lakes; (4) machine or deep learning methods are limited by coarse temporal resolution due to cloud contamination of satellite imagery, and lack of interpretability[17]. The storage changes of endorheic lakes accounted for 95–100% (161.9±14 Gt) of the total lake change observed from the 1970s to 2020, while exorheic lakes remained relatively stable (7.8±5.8 Gt)[21]. Therefore, we developed a data-driven, generalized modelling framework specifically for endorheic lakes to model their future annual changes, including lake surface area, water level, and lake water storage (Extended Data Fig. 2). Lake changes are mainly controlled by four dominant forcings: precipitation, glacier meltwater (Supplementary Text2), land evapotranspiration (Supplementary Text3), and lake evaporation[7,62]. The framework consists of two main steps: (1) projecting future changes in lake storage in response to climate change (Extended Data Fig. 2a), and (2) integrating inundation models and digital elevation models (DEMs), considering lake connectivity, to estimate actual surface area, water level, and actual lake storage (Extended Data Fig. 2b).

Step 1 of the modelling framework defines the concept of a stable period, where the size of the lake remains relatively constant during the beginning and end years of this period, allowing for fluctuations in lake size during this period (Extended Data Fig. 2a). The stable period can vary for each lake and was determined based on the changes in lake area from 1988 to 2018. Lakes on the TP experienced a contraction from the 1970s to 1995, followed by a significant expansion from 1995 to 2020. Most lakes have a stable period around 1995, such as the stable period 1989–1995 for Selin co. However, there are also some lakes that have a stable period after 2000, such as Peiku Co for 2008–2015. During the stable period, the lake is in a state of equilibrium, and then the equilibrium states of each factor are calculated as follows:

$$\bar{x}^k = \sum_{i=t1}^{t2} x_i^k / n \quad (4)$$

where k is the kth variable, including land precipitation (P_l), glacier meltwater (G), land evapotranspiration (ET), lake surface precipitation (P_w), and lake surface evaporation (E), respectively. $t1$ and $t2$ represent the start and end years of the stable period, n is the number of years in the stable period and i represents the years within the stable period. Furthermore, a concept of a change period is defined, which refers to the period outside the stable period for which lake storage data are available, mainly after 1990. The anomaly relative to the equilibrium state is calculated for each contributing factor during the change period as follows:

$$\delta x_i^k = x_i^k - \bar{x}^k \quad (5)$$

where i represents the years within the change period. Subsequently, the annual cumulative anomalies relative to the equilibrium state (Eq. 4) for each contribution factor were calculated, starting from the first year of the change period as follows:

$$X_i^k = \sum_{i=c1}^{2018} \delta x_i^k \quad (6)$$

where $c1$ represents the starting years of the change period, the form of each contribution factor can be expressed as land precipitation (PL_i^{cum}), glacier meltwater (G_i^{cum}), land evapotranspiration (ET_i^{cum}), lake surface precipitation (PW_i^{cum}), and lake surface evaporation (E_i^{cum}), respectively. Furthermore, we also calculated the annual cumulative changes in lake storage starting from the first year of the change period as follows:

$$V_i^{cum} = \sum_{i=c1}^{2018} (V_i - V_{i-1}) \quad (7)$$

By integrating the cumulative changes in lake storage and the cumulative anomalies relative to the equilibrium state for each contribution factor calculated from Eq. 6, the lake storage modelling framework can be expressed as:

$$V_i^{cum} = \alpha(\theta(PL_i^{cum} + G_i^{cum} - ET_i^{cum}) + PW_i^{cum} - E_i^{cum}) + \beta \quad (8)$$

Eq. 8 can be decomposed into the following two parts:

$$U_i = \theta(PL_i^{cum} + G_i^{cum} - ET_i^{cum}) + PW_i^{cum} - E_i^{cum} \quad (9)$$

$$V_i^{cum} = \alpha(U_i) + \beta \quad (10)$$

where $PL_i^{cum} + G_i^{cum} - ET_i^{cum}$ represents the land component, which includes the combined contributions of surface runoff, soil water, and groundwater to the lake change. θ is a land-specific parameter. $PW_i^{cum} - E_i^{cum}$ represents the lake surface component. U_i denotes a variable that integrates land surface precipitation, land evapotranspiration, glacier meltwater, lake surface precipitation, and lake surface evaporation, and is considered as net input.

The parameters in Eq. 8 were trained for each lake based on historical lake storage changes. Initially, the parameter θ was set to a fixed value of 1, and then α and β were determined using the Theil-Sen nonparametric method. If the R^2 value between α and β *was* greater than or equal to 0.60, the constructed model was used to estimate future changes in lake storage. However, if the R^2 value was less than 0.6, the parameter θ was adjusted in steps of 0.01 between 0.9 and 1.1, and then the Theil-Sen nonparametric method was used again to determine the α and β until the R^2 exceeded 0.60. If the R^2 remained consistently below 0.6, the lake was extrapolated based on the ratio of the average storage change of the nearest five lakes. It is worth emphasizing that U_i and V_i^{cum} showed a highly robust linear synchronization, which was prevalent among endorheic lakes on the TP (Extended Data Fig. 9a, Supplementary Fig. S10). The established model for each lake was then used to project future changes in lake storage in response to climate change by inputting the cumulative anomalies relative to the equilibrium state for each contribution factor from 2021 to 2100.

In step 2 of modelling framework (Extended Data Fig. 2b), the inundation model and DEM were combined, considering the connectivity of lakes[63], to accurately estimate the actual lake storage, water level, and surface area. If a lake continues to expand in the future until it reaches the lowest point of the basin boundary, it will overflow from its basin and flow into adjacent lakes, resulting in a stable phase. Conversely, lakes that receive overflow recharge from other lakes will experience accelerated expansion. Therefore, the constraint of topography on future lake change is essential.

NASADEM (30 m pixel size) was selected to estimate the distribution of the projected lake water volume changes because it was acquired instantaneously (11-day mission in February 2000) and has better accuracy compared to other available 30 m DEMs[64,65]. First, considering that the NASADEM corresponds to the year 2000, the average elevation of the lake boundary in 2020 was extracted from the NASADEM and then was used to replace all the elevations within the lake boundary in 2020. Then, using the regional growth algorithm with the center of the lake as the seed point, a growth of 60 m was initiated to determine the corresponding changes in area, water level, and water storage for each step of 1 m growth. Additionally, the maximum storage capacity of the lake basin was determined and compared to the projected water storage from Step 1, to determine whether the lake would overflow from the basin or receive inflows from other lakes. Furthermore, the estimated water storage in Step 1 was also matched with the water storage change corresponding to the 1–60 m growth to determine the flow paths of water between adjacent lakes each year, redistributing the water storage and obtaining the actual annual variations in lake storage, as well as the corresponding annual water level and area under the SSP1-2.6, SSP2-4.5, and SSP5-8.5 scenarios. For lakes experiencing a reduction in size, the approach involves utilizing a robust empirical linear volume-area-level relationship[21], when the projected water volume change is less than the volume loss recorded between 2000 and 2020. The lake outlines from 2020 were used to conservatively estimate the potential impact of lake inundation. On the contrary, when the projected lake volume change is greater than the recorded volume loss between 2000 and 2020, the estimation of the extent is determined through the application of a regional growth algorithm. Further details on the method for analyzing the impacts of lake changes, auxiliary data and the attribution of future lake changes are available in the Supplementary Texts6–8.

Validation and error estimation of future lake modelling

To evaluate the robustness of our approach, the R^2 between U_i (net input) and V_i^{cum} (accumulated lake storage) was employed to assess the generalizability of the framework (see ‘Development of future lake modelling framework’ in Method). The modelling framework developed in this study using four drivers performs well, explaining more than 94% of the historical lake storage change in ~70% of the lakes, with a uniform distribution across the TP (Extended Data Fig. 9). Among the 307 endorheic lakes, there were 214, 189, 154, and 91 lakes with R^2 higher than 0.60 (70%), 0.70 (62%), 0.80 (50%), and 0.90 (30%), respectively, which could explain 94%, 92%, 85%, and 61% of the historical lake storage changes, respectively (Extended Data Fig. 9). Furthermore, the performance of the modelling framework varies among lakes of different sizes, with larger lakes performing better, leading to a higher proportion of lakes and water storage that can be explained. In addition, the samples for each lake were split in time, with the initial 70% allocated for model training and the remaining 30% for validation. The model's performance was assessed using the correlation coefficient (R), Bias, and RMSE. The simulated and observed changes in lake water storage showed good agreement during the validation period, with an overall R of 0.97 and a bias of 0.05 (Extended Data Fig. 10). The correlation coefficients and bias distribution for different lakes also demonstrate good accuracy of the modelling framework.

The Bootstrap method, a non-parametric approach to estimating confidence intervals of sample statistics through repeated resampling of the original dataset, was used to assess the uncertainty of projected future lake storage changes. For each lake, the historical data used for parameter training were resampled with replacement 1000 times, with each sample comprising 50% of the total dataset. These 50% samples were used to train 1000 sets of corresponding models, which were then used to estimate 1000 sets of future lake storage changes. Finally, the 95% confidence interval of the annual results was taken as the uncertainty of the estimate. Subsequently, the uncertainty of lake storage changes was converted into the uncertainty of water level and area, for example, if the error of lake storage for a given year is ~1 Gt, the uncertainty in water level and area corresponds to the changes in water level and area for that year. The uncertainty of submerged roads and grasslands was estimated based on the lake area. First, the submerged roads and grasslands corresponding to the area changes from 2021 to 2100 were calculated. Then, the uncertainty in area for each year was proportionally converted to the uncertainty in submerged roads and grasslands.

Limitations and uncertainties of future lake modelling

Our model does not account for the effects of thermodynamic changes due to mixing regimes resulting from basin reorganization and lake mergers in future changes. Given the 30 m spatial resolution of NASADEM, changes in lake boundaries within a year are occasionally less than one pixel, in which case the previous year's boundaries were used. Selin Co, which has the largest lake surface area in Tibet and the largest historical extent change on the TP, was selected as a case study to evaluate the impact of DEM accuracy on the projected lake water volume distribution. The DEM accuracy could introduce a small uncertainty due to the influence of elevation uncertainty, especially at the lake basin outlet (Supplementary Fig. S11). However, our analysis showed only a small discrepancy in the projected lake volume change from NASADEM compared to the high-accuracy AW3D30 DEM[66]. The time series of future volume changes between them are in good agreement (R>0.98). Furthermore, the DEM-derived lake volume trends show small errors (R^2=0.97 and bias=~5%) compared to the altimetry-derived trends for 18 Tibetan lakes[8]. It is important to emphasize that our projections are highly dependent on the climate projection used under the CMIP SSP scenarios. However, due to differences in the representation of physical processes, parameterization schemes, and the ability to simulate climate systems across climate models, there are discrepancies in projections under the same scenario. To reduce the uncertainty in future projections, the average of multiple models was used.

A direct estimate of the groundwater contribution to lake change is limited by the lack of groundwater observations. Basin-wide groundwater change in the inner TP, estimated from decomposed terrestrial water storage based on GRACE observations, suggests a significant but smaller magnitude water mass gain relative to lake change[7]. Our model accounts for groundwater contribution indirectly, with P-ET+G representing the combined contributions of surface runoff, soil water, and groundwater without distinguishing their individual effects on lakes. In addition, our model does not include the influence of permafrost on future lake changes due to the current limited understanding of the freeze-thaw and hydrothermal processes of permafrost on the TP[67], which could also introduce uncertainties in future lake modelling. However, we consider this to be somewhat limited due to the small contribution of ground ice meltwater to the historical increase in lake water storage[7,68].

Data availability

The lake boundaries from 2021 to 2100 produced by this study are available at https://doi.org/10.6084/m9.figshare.24873747. Precipitation and evapotranspiration from ERA5-Land can be accessed at https://www.ecmwf.int/en/era5-land. TPHiPr precipitation dataset is acquired at https://doi.org/10.11888/Atmos.tpdc.272763. Noah_GL can be accessed at https://disc.gsfc.nasa.gov/datasets/GLDAS_NOAH025_M_2.0/summary?keywords=GLDAS_NOAH025_M_2.0. GLEAM can be accessed at https://www.gleam.eu. CMFD can be accessed at http://poles.tpdc.ac.cn/en/data/8028b944-daaa-4511-8769-965612652c49. NASADEM data are downloaded from https://search.earthdata.nasa.gov.

HydroSHED can be accessed at https://www.hydrosheds.org. The outputs of CMIP6 ESMs can be access at https://esgf-node.llnl.gov/search/cmip6. OpenStreetMap can be accessed at https://www.openstreetmap.org. Settlement data can be accessed at http://www.webmap.cn.

Code availability

The codes associated with this study are available on request from the corresponding authors upon request.

References

47 Crétaux, J. F. *et al.* Lake Volume Monitoring from Space. *Surveys in Geophysics* **37**, 269-305, doi:10.1007/s10712-016-9362-6 (2016).

48 Crétaux, J. F. *et al.* SOLS: A lake database to monitor in the Near Real Time water level and storage variations

from remote sensing data. *Advances in Space Research* **47**, 1497-1507, doi:10.1016/j.asr.2011.01.004 (2011).
49 Zhao, R. *et al.* Annual 30-m big Lake Maps of the Tibetan Plateau in 1991-2018. *Sci Data* **9**, 164, doi:10.1038/s41597-022-01275-9 (2022).
50 Li, X. *et al.* High-temporal-resolution water level and storage change data sets for lakes on the Tibetan Plateau during 2000–2017 using multiple altimetric missions and Landsat-derived lake shoreline positions. *Earth Syst. Sci. Data* **11**, 1603-1627, doi:10.5194/essd-11-1603-2019 (2019).
51 Muñoz-Sabater, J. *et al.* ERA5-Land: a state-of-the-art global reanalysis dataset for land applications. *Earth System Science Data* **13**, 4349-4383, doi:10.5194/essd-13-4349-2021 (2021).
52 Wu, X., Su, J., Ren, W., Lü, H. & Yuan, F. Statistical comparison and hydrological utility evaluation of ERA5-Land and IMERG precipitation products on the Tibetan Plateau. *Journal of Hydrology* **620**, doi:10.1016/j.jhydrol.2023.129384 (2023).
53 Jiang, Y. *et al.* TPHiPr: a long-term (1979－2020) high-accuracy precipitation dataset (1／30°, daily) for the Third Pole region based on high-resolution atmospheric modeling and dense observations. *Earth System Science Data* **15**, 621-638, doi:10.5194/essd-15-621-2023 (2023).
54 He, J. *et al.* The first high-resolution meteorological forcing dataset for land process studies over China. *Sci Data* **7**, 25, doi:10.1038/s41597-020-0369-y (2020).
55 Wang, B., Ma, Y., Su, Z., Wang, Y. & Ma, W. Quantifying the evaporation amounts of 75 high-elevation large dimictic lakes on the Tibetan Plateau. *Sci Adv* **6**, eaay8558, doi:10.1126/sciadv.aay8558 (2020).
56 La, Z. *The Response of Lake Evaporation to Climate Change and Its Impact on Lake Water Balance Change for Large Lakes in the Tibetan Plateau*, University of Chinese Academy of Sciences, (2017).
57 Grossman, R. L. *et al.* Reservoir Evaporation in the Western United States: Current Science, Challenges, and Future Needs. *Bulletin of the American Meteorological Society* **99**, 167-187, doi:10.1175/bams-d-15-00224.1 (2018).
58 Penman, H. L. Natural evaporation from open water, bare soil and grass. *Proceedings of the Royal Society of London. Series A. Mathematical and Physical Sciences* **193**, 120-145 (1948).
59 Zhao, G., Li, Y., Zhou, L. & Gao, H. Evaporative water loss of 1.42 million global lakes. *Nat Commun* **13**, 3686, doi:10.1038/s41467-022-31125-6 (2022).
60 Zhou, J. *et al.* Exploring the water storage changes in the largest lake (Selin Co) over the Tibetan Plateau during 2003-2012 from a basin-wide hydrological modeling. *Water Resources Research* **51**, 8060-8086, doi:10.1002/2014wr015846 (2015).
61 Zhang, Y., Ohata, T., Ersi, K. & Tandong, Y. Observation and estimation of evaporation from the ground surface of the cryosphere in eastern Asia. *Hydrological processes* **17**, 1135-1147, doi:10.1002/hyp.1183 (2003).
62 Zhou, J. *et al.* Quantifying the major drivers for the expanding lakes in the interior Tibetan Plateau. *Science Bulletin* **67**, 474-478, doi:10.1016/j.scib.2021.11.010 (2021).
63 Liu, K. *et al.* Ongoing drainage reorganization driven by rapid lake growths on the Tibetan Plateau. *Geophysical Research Letters* **48**, doi:10.1029/2021gl095795 (2021).
64 Li, H., Zhao, J., Yan, B., Yue, L. & Wang, L. Global DEMs vary from one to another: an evaluation of newly released Copernicus, NASA and AW3D30 DEM on selected terrains of China using ICESat-2 altimetry data. *International Journal of Digital Earth* **15**, 1149-1168, doi:10.1080/17538947.2022.2094002 (2022).
65 Uuemaa, E., Ahi, S., Montibeller, B., Muru, M. & Kmoch, A. Vertical Accuracy of Freely Available Global Digital Elevation Models (ASTER, AW3D30, MERIT, TanDEM-X, SRTM, and NASADEM). *Remote Sensing* **12**, doi:10.3390/rs12213482 (2020).
66 Liu, K. *et al.* Global open-access DEM performances in Earth's most rugged region High Mountain Asia: A multi-level assessment. *Geomorphology* **338**, 16-26, doi:10.1016/j.geomorph.2019.04.012 (2019).

67 Ni, J. *et al.* Simulation of the Present and Future Projection of Permafrost on the Qinghai - Tibet Plateau with Statistical and Machine Learning Models. *Journal of Geophysical Research: Atmospheres* **126**, doi:10.1029/2020jd033402 (2021).

68 Wang, L. *et al.* Contribution of ground ice melting to the expansion of Selin Co (lake) on the Tibetan Plateau. *The Cryosphere* **16**, 2745-2767, doi:10.5194/tc-16-2745-2022 (2022).

69 Li, Z., Sun, Y., Li, T., Ding, Y. & Hu, T. Future Changes in East Asian Summer Monsoon Circulation and Precipitation Under 1.5 to 5 °C of Warming. *Earth's Future* **7**, 1391-1406, doi:10.1029/2019ef001276 (2019).

70 Katzenberger, A., Schewe, J., Pongratz, J. & Levermann, A. Robust increase of Indian monsoon rainfall and its variability under future warming in CMIP6 models. *Earth System Dynamics* **12**, 367-386, doi:10.5194/esd-12-367-2021 (2021).

71 Li, Y. *et al.* Westerly jet stream controlled climate change mode since the Last Glacial Maximum in the northern Qinghai-Tibet Plateau. *Earth and Planetary Science Letters* **549**, doi:10.1016/j.epsl.2020.116529 (2020).

72 *Randolph Glacier Inventory—A Dataset of Global Glacier Outlines Version 6.0 (NSIDC, 2017)*, <https://doi.org/10.7265/4m1f-gd79> (2017).

Additional information

Supplementary information. The online version contains supplementary material available at

Correspondence and requests for materials should be addressed to G. Zhang.

Peer review information

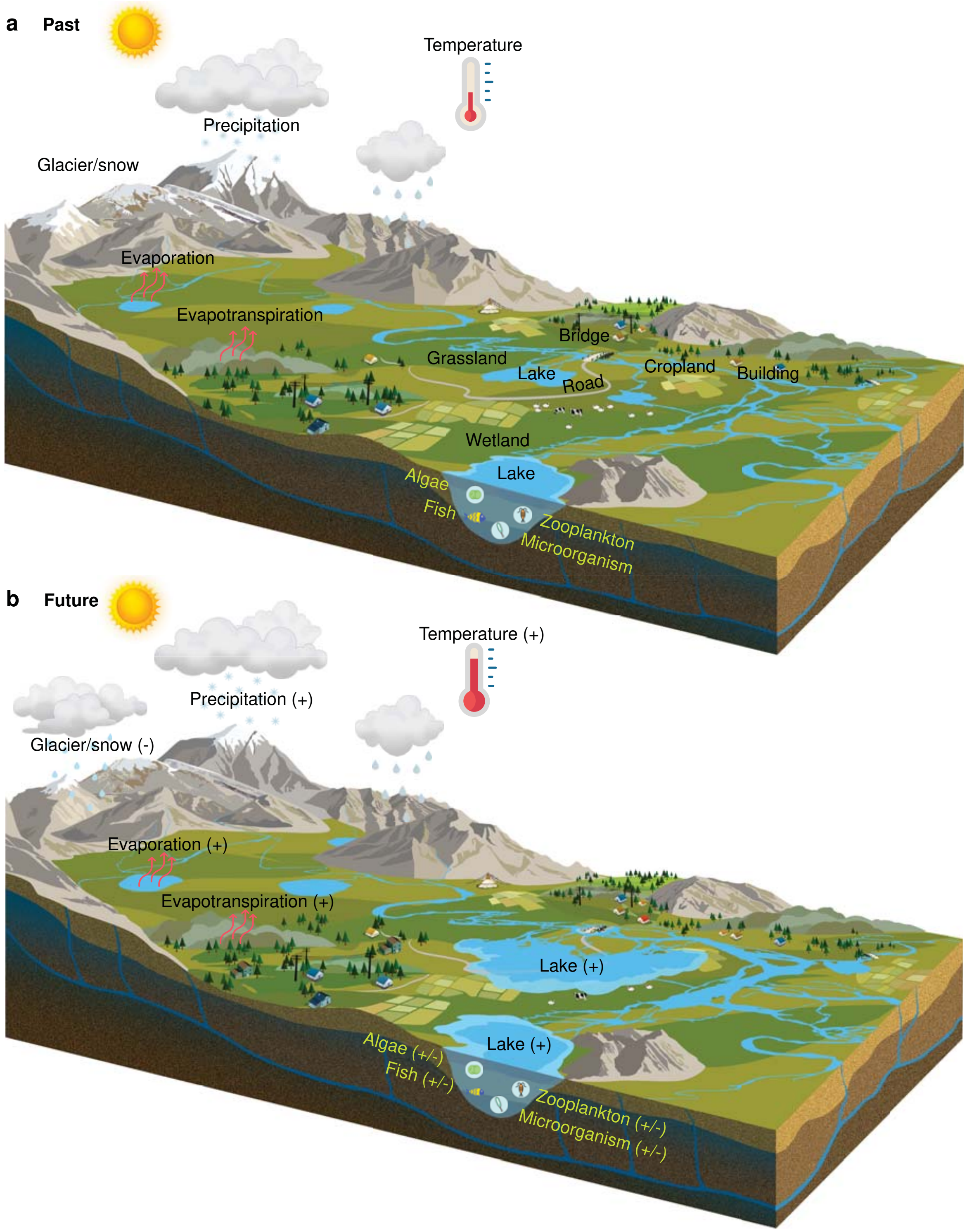

a Past
Temperature
Precipitation
Glacier/snow
Evaporation
Evapotranspiration
Bridge
Grassland
Lake
Road
Cropland
Building
Wetland
Lake
Algae
Fish
Zooplankton
Microorganism
b Future
Temperature (+)
Precipitation (+)
Glacier/snow (-)
Evaporation (+)
Evapotranspiration (+)
Lake (+)
Lake (+)
Algae (+/-)
Fish (+/-)
Zooplankton (+/-)
Microorganism (+/-)

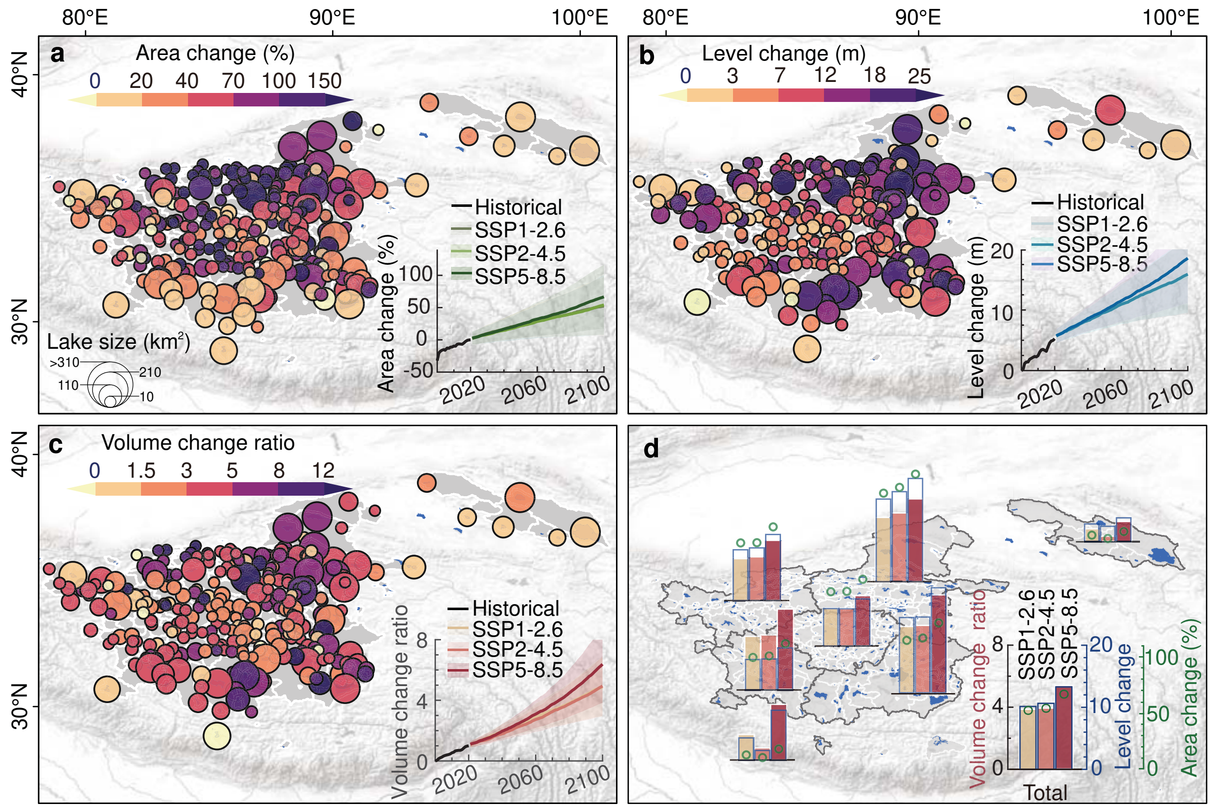
80°E
90°E
100°E
40°N
30°N
a
Area change (%)
0 20 40 70 100 150
Lake size (km2)
>310
210
110
10
Historical
SSP1-2.6
SSP2-4.5
SSP5-8.5
Area change (%)
100
50
0
-50
2020
2060
2100
b
Level change (m)
0 3 7 12 18 25
Level change (m)
20
10
0
c
Volume change ratio
0 1.5 3 5 8 12
Volume change ratio
8
4
0
d
SSP1-2.6
SSP2-4.5
SSP5-8.5
Volume change ratio
Level change
Area change (%)
Total

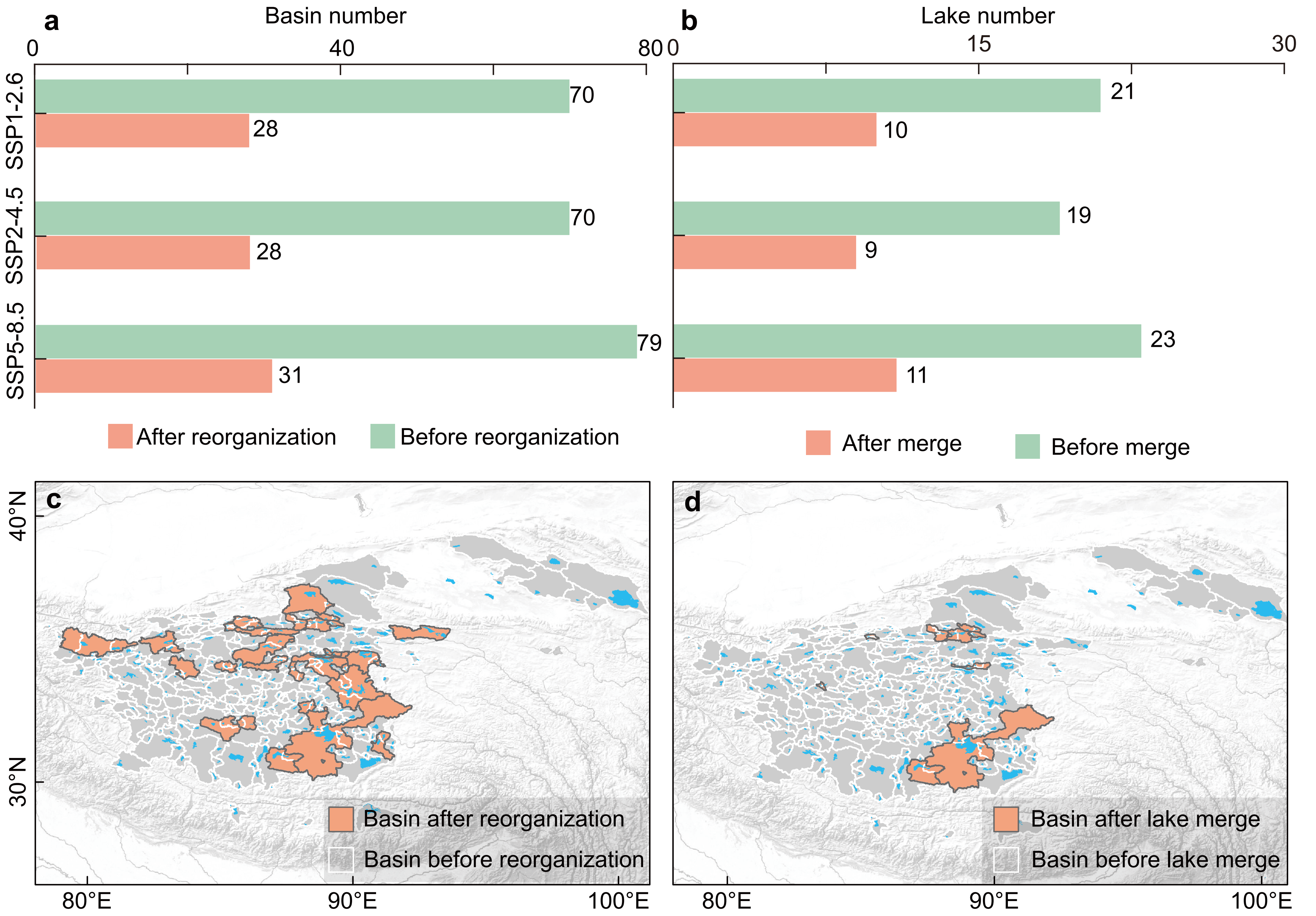
a
Basin number
0
40
80
SSP1-2.6
SSP2-4.5
SSP5-8.5
70
28
70
28
79
31
After reorganization
Before reorganization
b
Lake number
0
15
30
21
10
19
9
23
11
After merge
Before merge
c
40°N
30°N
Basin after reorganization
Basin before reorganization
80°E
90°E
100°E
d
Basin after lake merge
Basin before lake merge
80°E
90°E
100°E

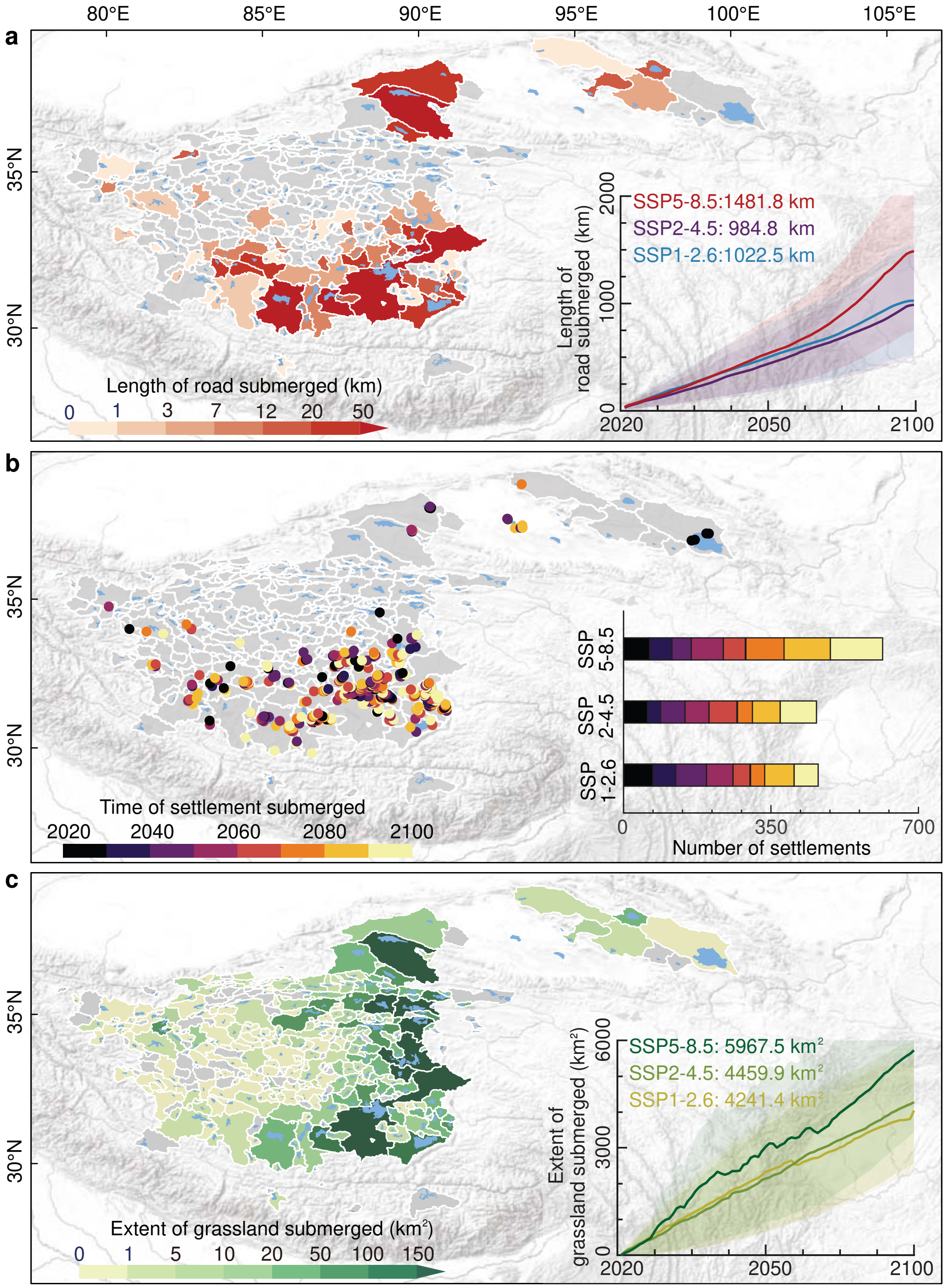
80°E
85°E
90°E
95°E
100°E
105°E
35°N
30°N
a
Length of road submerged (km)
0
1
3
7
12
20
50
Length of road submerged (km)
SSP5-8.5:1481.8 km
SSP2-4.5: 984.8 km
SSP1-2.6:1022.5 km
0
1000
2000
2020
2050
2100
b
Time of settlement submerged
2020
2040
2060
2080
2100
SSP 5-8.5
SSP 2-4.5
SSP 1-2.6
0
350
700
Number of settlements
c
Extent of grassland submerged (km²)
0
1
5
10
20
50
100
150
Extent of grassland submerged (km²)
SSP5-8.5: 5967.5 km²
SSP2-4.5: 4459.9 km²
SSP1-2.6: 4241.4 km²
0
3000
6000
2020
2050
2100

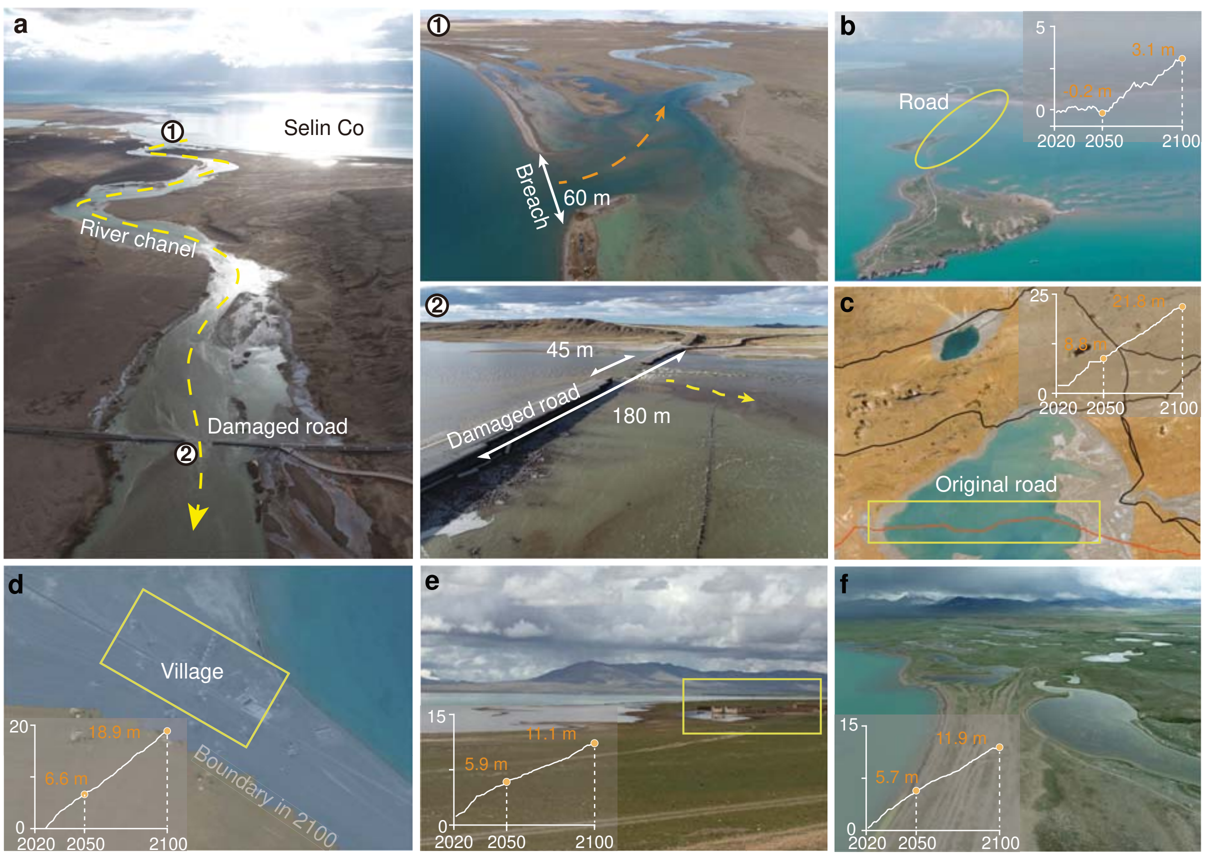

a
Selin Co
River chanel
Damaged road
①
Breach
60 m
b
Road
5
0
-0.2 m
3.1 m
2020
2050
2100
②
45 m
Damaged road
180 m
c
25
0
8.8 m
21.8 m
2020
2050
2100
Original road
d
Village
Boundary in 2100
20
0
6.6 m
18.9 m
2020
2050
2100
e
15
0
5.9 m
11.1 m
2020
2050
2100
f
15
0
5.7 m
11.9 m
2020
2050
2100

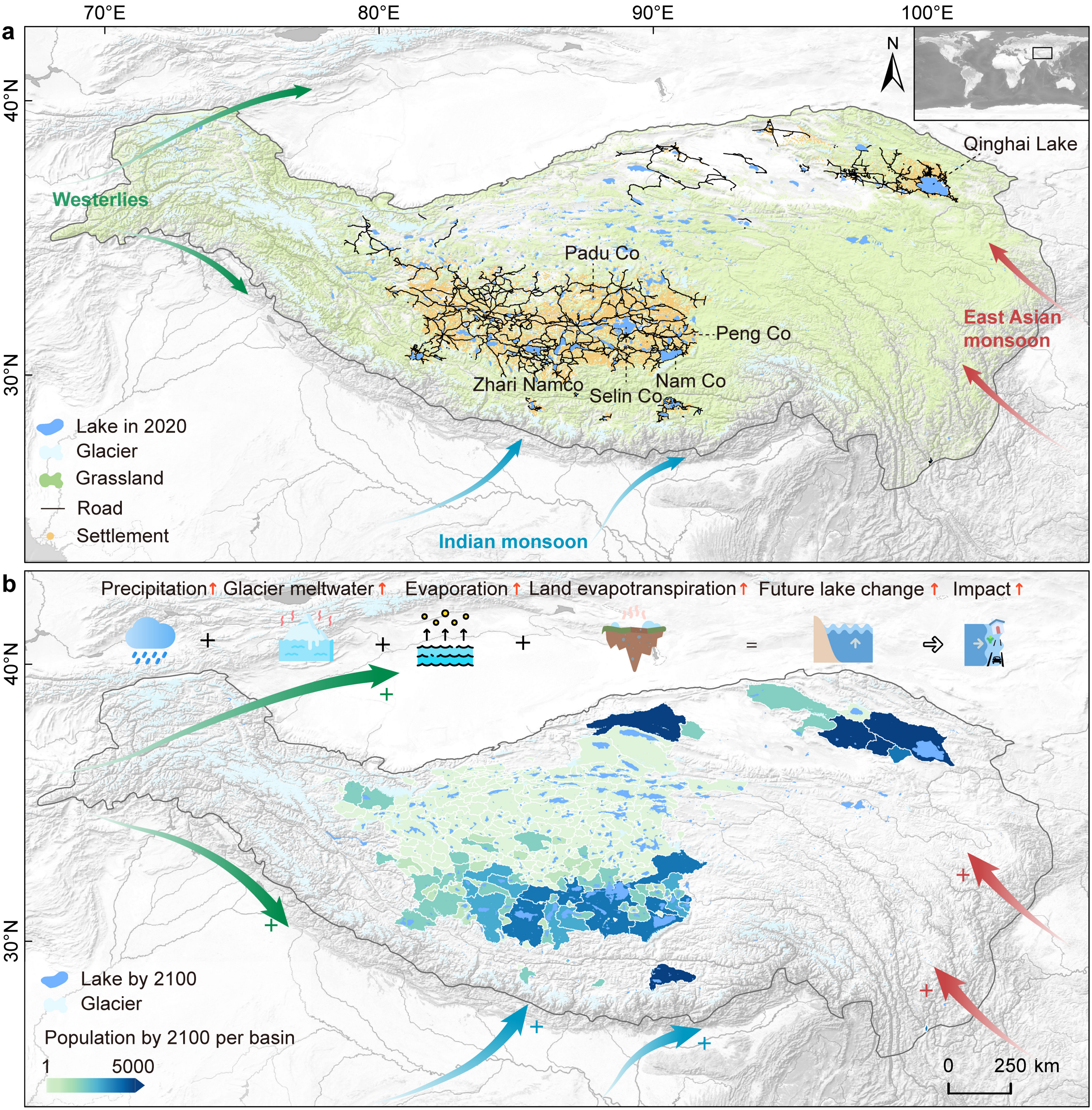

a
70°E
80°E
90°E
100°E
40°N
30°N
N
Qinghai Lake
Westerlies
Padu Co
Peng Co
East Asian monsoon
Zhari Namco
Selin Co
Nam Co
Lake in 2020
Glacier
Grassland
Road
Settlement
Indian monsoon
b
Precipitation↑ Glacier meltwater↑ Evaporation↑ Land evapotranspiration↑ Future lake change↑ Impact↑
+
+
+
=
40°N
30°N
Lake by 2100
Glacier
Population by 2100 per basin
1
5000
0
250 km

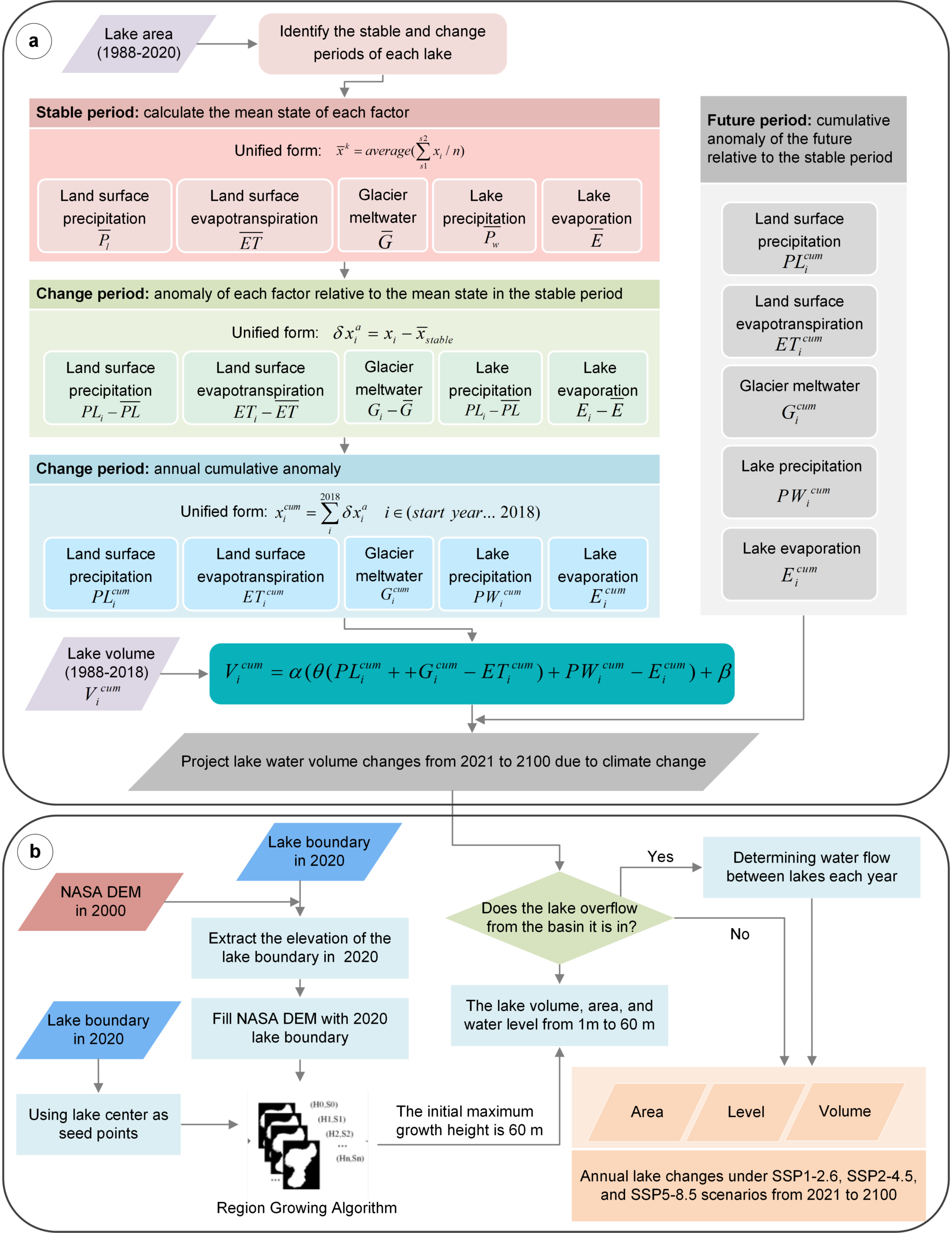
a
Lake area (1988-2020)
Identify the stable and change periods of each lake
Stable period: calculate the mean state of each factor
Unified form: $\bar{x}^k = average(\sum_{s1}^{s2} x_i / n)$
Land surface precipitation $\overline{P_l}$
Land surface evapotranspiration $\overline{ET}$
Glacier meltwater $\overline{G}$
Lake precipitation $\overline{P_w}$
Lake evaporation $\overline{E}$
Change period: anomaly of each factor relative to the mean state in the stable period
Unified form: $\delta x_i^a = x_i - \bar{x}_{stable}$
Land surface precipitation $PL_i - \overline{PL}$
Land surface evapotranspiration $ET_i - \overline{ET}$
Glacier meltwater $G_i - \overline{G}$
Lake precipitation $PL_i - \overline{PL}$
Lake evaporation $E_i - \overline{E}$
Change period: annual cumulative anomaly
Unified form: $x_i^{cum} = \sum_i^{2018} \delta x_i^a \quad i \in (start\ year ... 2018)$
Land surface precipitation PL_i^{cum}
Land surface evapotranspiration ET_i^{cum}
Glacier meltwater G_i^{cum}
Lake precipitation PW_i^{cum}
Lake evaporation E_i^{cum}
Future period: cumulative anomaly of the future relative to the stable period
Land surface precipitation PL_i^{cum}
Land surface evapotranspiration ET_i^{cum}
Glacier meltwater G_i^{cum}
Lake precipitation PW_i^{cum}
Lake evaporation E_i^{cum}
Lake volume (1988-2018) V_i^{cum}
$V_i^{cum} = \alpha(\theta(PL_i^{cum} + +G_i^{cum} - ET_i^{cum}) + PW_i^{cum} - E_i^{cum}) + \beta$
Project lake water volume changes from 2021 to 2100 due to climate change
b
NASA DEM in 2000
Lake boundary in 2020
Extract the elevation of the lake boundary in 2020
Fill NASA DEM with 2020 lake boundary
Lake boundary in 2020
Using lake center as seed points
(H0,S0)
(H1,S1)
(H2,S2)
(Hn,Sn)
Region Growing Algorithm
The initial maximum growth height is 60 m
Does the lake overflow from the basin it is in?
Yes
No
Determining water flow between lakes each year
The lake volume, area, and water level from 1m to 60 m
Area
Level
Volume
Annual lake changes under SSP1-2.6, SSP2-4.5, and SSP5-8.5 scenarios from 2021 to 2100

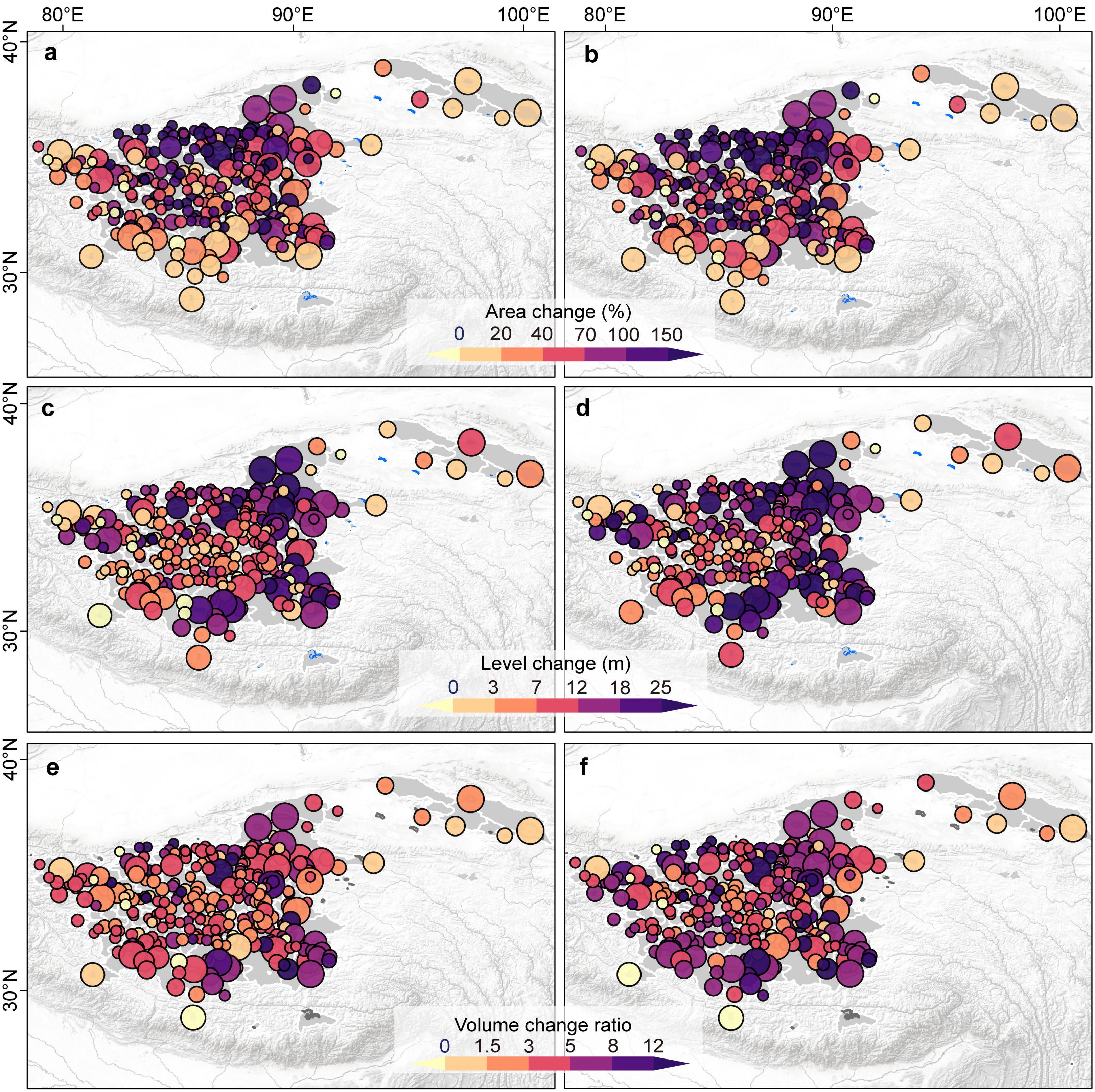

80°E
90°E
100°E
40°N
30°N
a
b
c
d
e
f
Area change (%)
0 20 40 70 100 150
Level change (m)
0 3 7 12 18 25
Volume change ratio
0 1.5 3 5 8 12

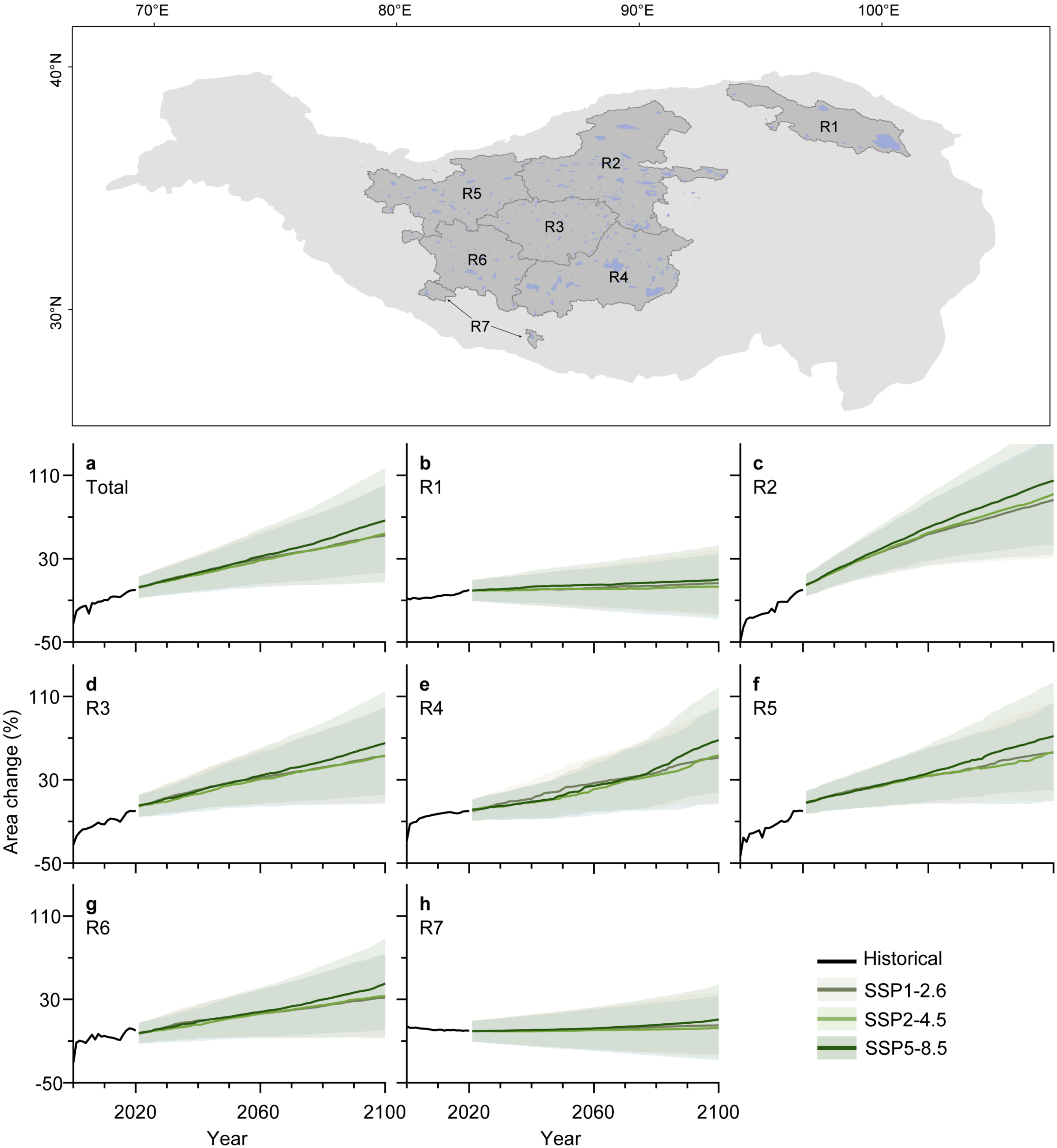

70°E
80°E
90°E
100°E
40°N
30°N
R1
R2
R3
R4
R5
R6
R7
a
Total
b
R1
c
R2
d
R3
e
R4
f
R5
g
R6
h
R7
110
30
-50
Area change (%)
2020
2060
2100
Year
Historical
SSP1-2.6
SSP2-4.5
SSP5-8.5

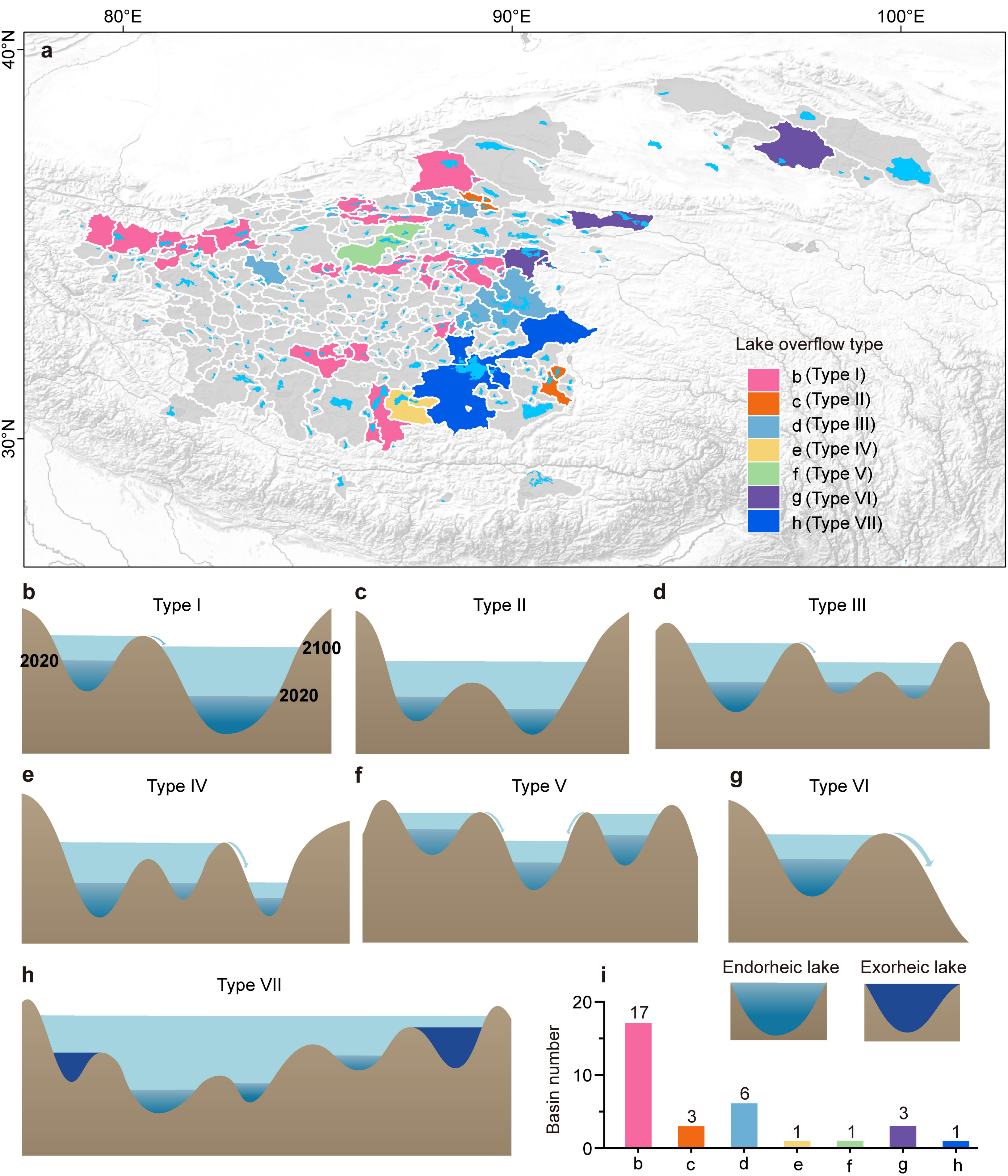

a
80°E
90°E
100°E
40°N
30°N
Lake overflow type
b (Type I)
c (Type II)
d (Type III)
e (Type IV)
f (Type V)
g (Type VI)
h (Type VII)
b
Type I
2020
2100
2020
c
Type II
d
Type III
e
Type IV
f
Type V
g
Type VI
h
Type VII
i
Endorheic lake
Exorheic lake
Basin number
0
10
20
17
3
6
1
1
3
1
b
c
d
e
f
g
h

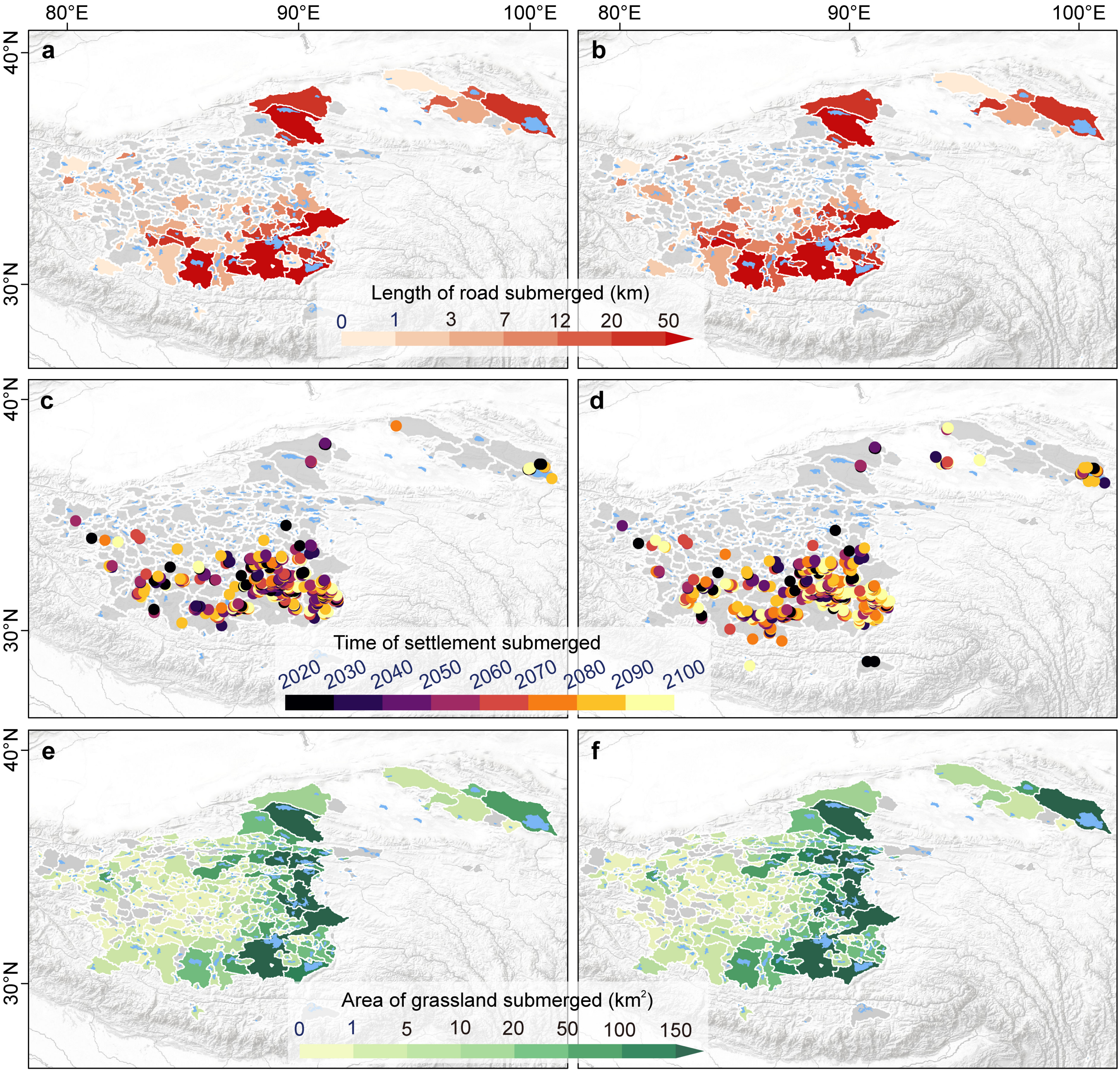

80°E
90°E
100°E
40°N
30°N
a
b
c
d
e
f
Length of road submerged (km)
0
1
3
7
12
20
50
Time of settlement submerged
2020
2030
2040
2050
2060
2070
2080
2090
2100
Area of grassland submerged (km²)
0
1
5
10
20
50
100
150

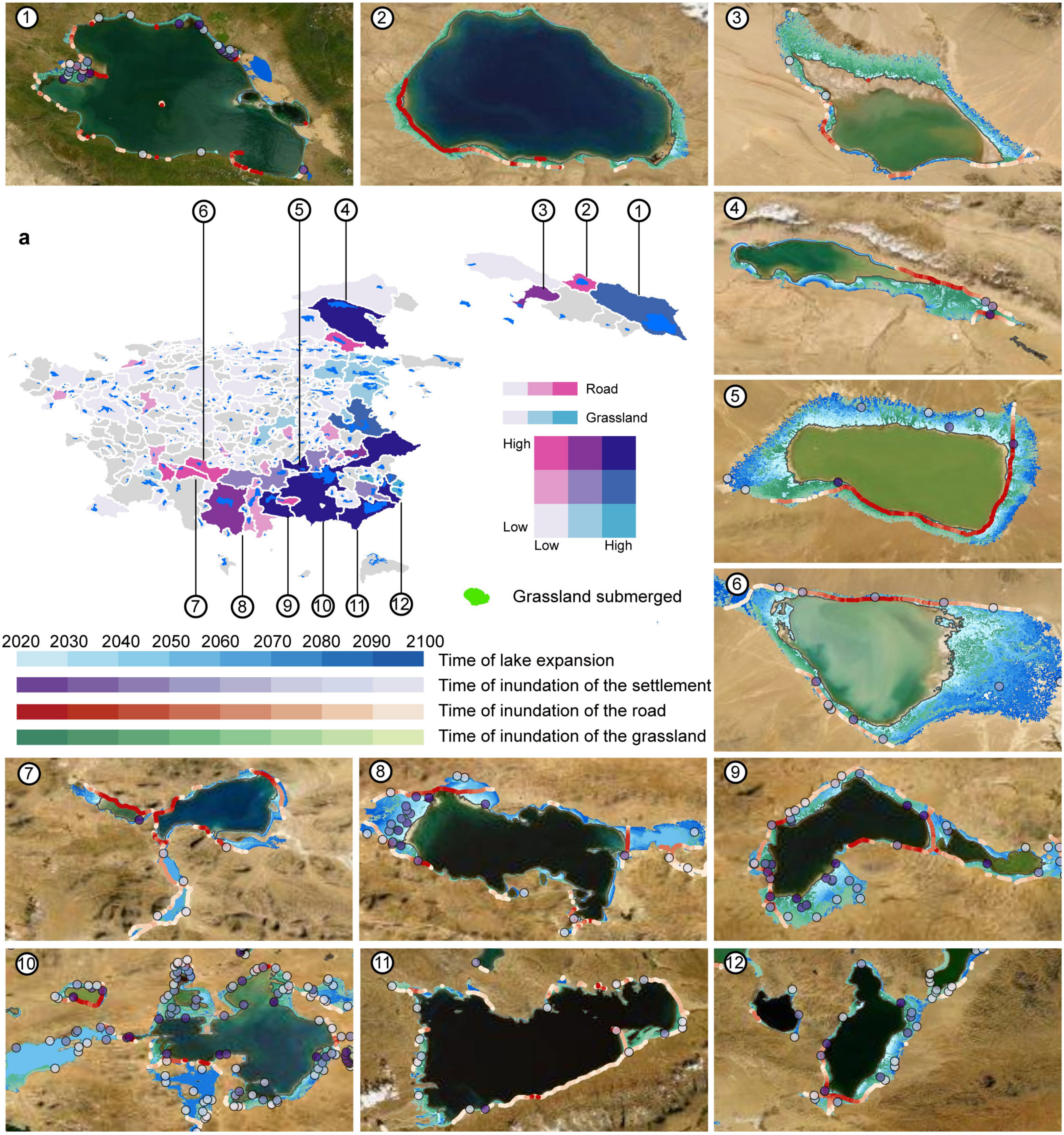

a
Road
Grassland
High
Low
Low
High
Grassland submerged
2020 2030 2040 2050 2060 2070 2080 2090 2100
Time of lake expansion
Time of inundation of the settlement
Time of inundation of the road
Time of inundation of the grassland

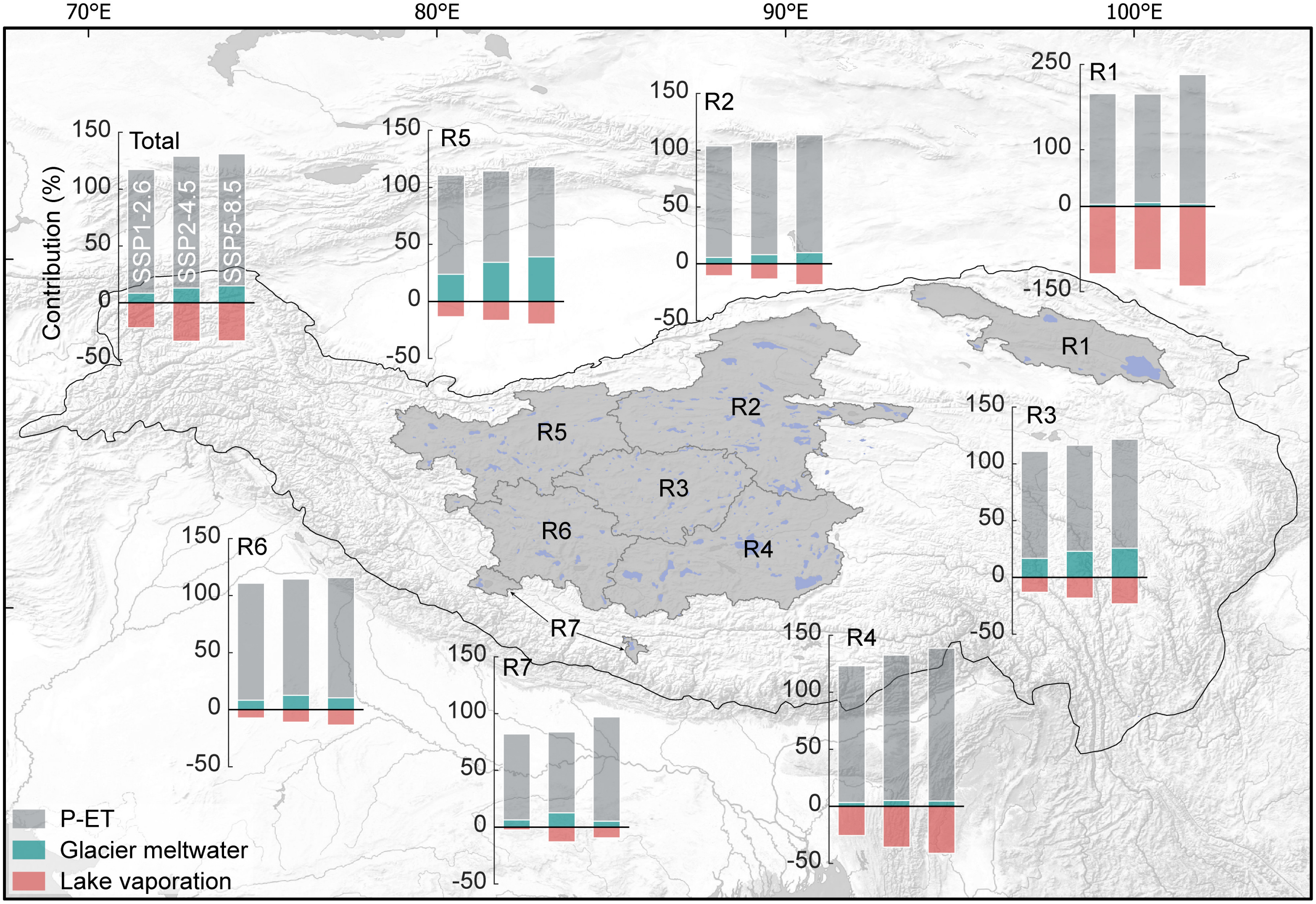
70°E
80°E
90°E
100°E
40°N
30°N
Contribution (%)
Total
SSP1-2.6
SSP2-4.5
SSP5-8.5
R1
R2
R3
R4
R5
R6
R7
P-ET
Glacier meltwater
Lake vaporation

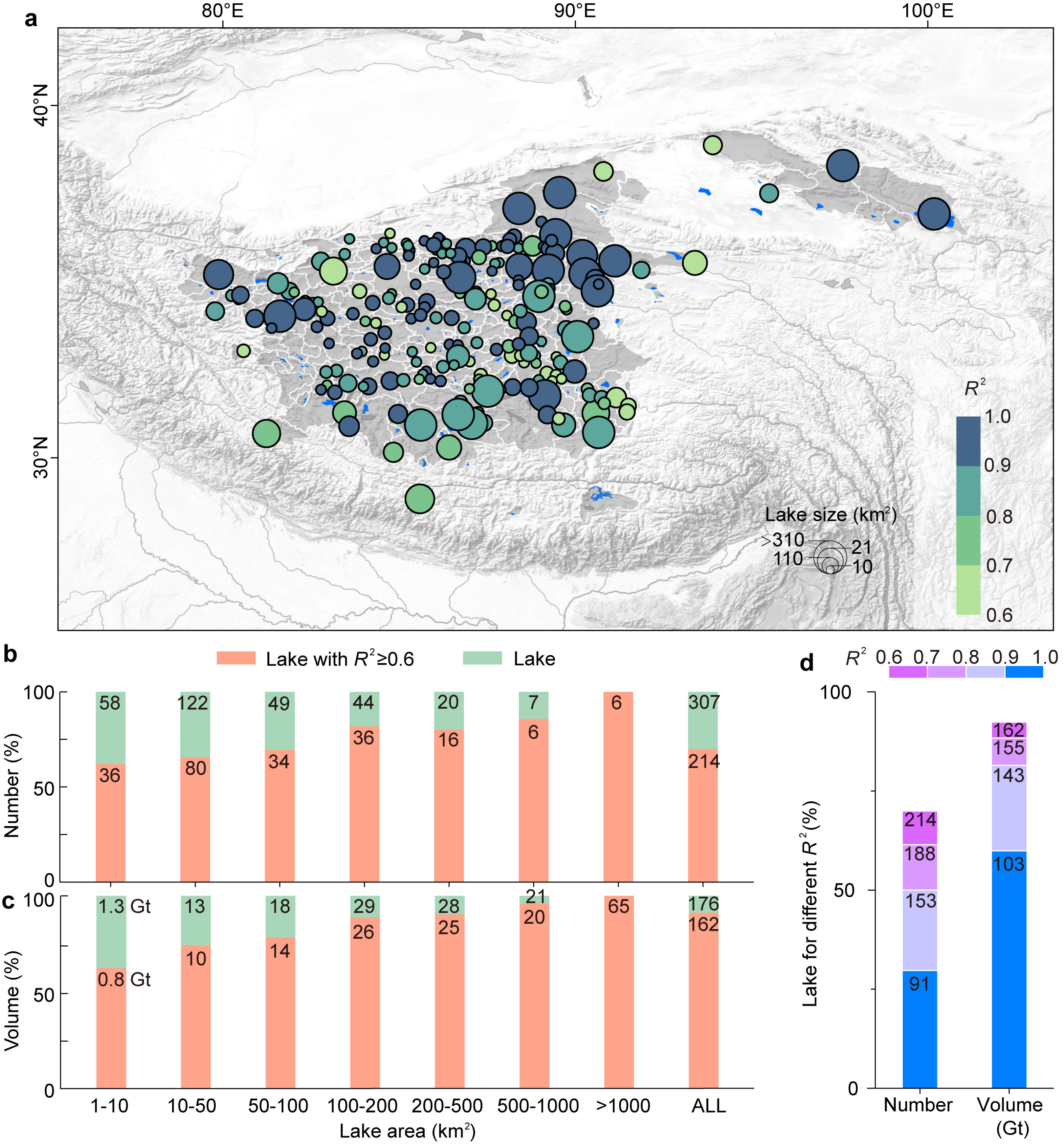
a
80°E
90°E
100°E
40°N
30°N
R^2
1.0
0.9
0.8
0.7
0.6
Lake size (km²)
>310
110
21
10
b
Lake with R^2≥0.6
Lake
Number (%)
100
50
0
58
36
122
80
49
34
44
36
20
16
7
6
6
307
214
c
Volume (%)
1.3 Gt
0.8 Gt
13
10
18
14
29
26
28
25
21
20
65
176
162
1-10
10-50
50-100
100-200
200-500
500-1000
>1000
ALL
Lake area (km²)
d
R^2 0.6 0.7 0.8 0.9 1.0
Lake for different R^2 (%)
214
188
153
91
162
155
143
103
Number
Volume (Gt)

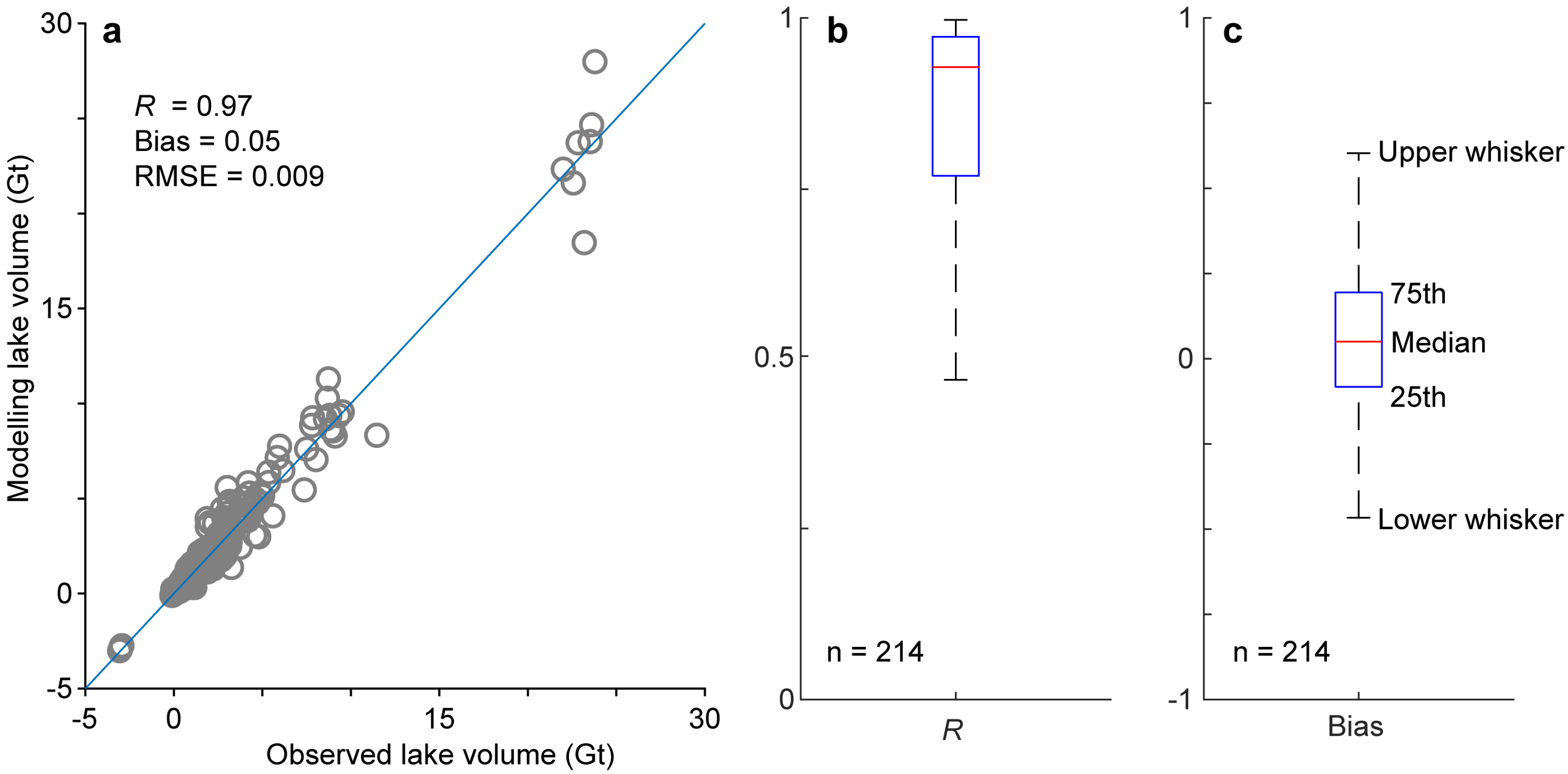
a
R = 0.97
Bias = 0.05
RMSE = 0.009
Modelling lake volume (Gt)
Observed lake volume (Gt)
30
15
0
-5
-5
0
15
30
b
1
0.5
0
n = 214
R
c
1
0
-1
Upper whisker
75th
Median
25th
Lower whisker
n = 214
Bias